Optical Wireless Communication Channel Measurements and Models

Ahmed Al-Kinani, Cheng-Xiang Wang, *Fellow, IEEE*, Li Zhou, and Wensheng Zhang, *Member, IEEE*

Abstract—**Optical wireless communications (OWCs) refer to wireless communication technologies which utilize optical carriers in infrared, visible light, or ultraviolet bands of electromagnetic spectrum. For the sake of an OWC link design and performance evaluation, a comprehensive understanding and an accurate prediction of link behavior are indispensable. Therefore, accurate and efficient channel models are crucial for the OWC link design. This paper first provides a brief history of OWCs. It also considers OWC channel scenarios and their utilization trade-off in terms of optical carrier, range, mobility, and power efficiency. Furthermore, the main optical channel characteristics that affect the OWC link performance are investigated. A comprehensive overview of the most important OWCs channel measurement campaigns and channel models, primarily for wireless infrared communications and visible light communications, are presented. OWCs channel models are further compared in terms of computation speed, complexity, and accuracy. The survey considers indoor, outdoor, underground, and underwater communication environments. Finally, future research directions in OWCs channel measurements and models are addressed.**

Index Terms—**Wireless infrared communications, visible light communications, optical wireless channel characteristics, optical wireless channel measurements, optical wireless channel models.**

I. Introduction

RADIO frequency (RF) wireless systems designers have been facing the continuously increasing demand for

A. Al-Kinani was with the Institute of Sensors, Signals and Systems, School of Engineering and Physical Sciences, Heriot-Watt University, Edinburgh EH14 4AS, U.K. He is now with the Technical Affairs Department, Iraqi Ministry of Communications, Baghdad 10013, Iraq (e-mail: aa1304@hw.ac.uk).

C.-X. Wang is with the Mobile Communications Research Laboratory, Southeast University, Nanjing 211189, China, and also with the Institute of Sensors, Signals and Systems, School of Engineering and Physical Sciences, Heriot-Watt University, Edinburgh EH14 4AS, U.K. (e-mail: chengxiang.wang@hw.ac.uk).

L. Zhou is with the School of Microelectronics, Shandong University, Shandong 250100, China (e-mail: zhou_li@sdu.edu.cn).

W. Zhang is with the Shandong Provincial Key Laboratory of Wireless Communication Technologies, School of Information Science and Engineering, Shandong University, Shandong 250100, China (e-mail: zhangwsh@sdu.edu.cn).

Digital Object Identifier 10.1109/COMST.2018.2838096

high capacity and high data rates required by new wireless applications. Therefore, researchers have been focusing on the fifth generation (5G) wireless communication systems that are expected to be deployed around 2020 [1]. Various potential promising technologies for 5G systems have been suggested, such as massive multiple-input multiple-output (MIMO) [2], cell densification, cognitive radio networks, and millimeter wave (mmWave) communications [3], [4]. Further shifting beyond mmWave frequencies, there is about 0.3 – 30000 THz of bandwidth that does not fall under the federal communications commission (FCC) regulations called optical spectrum [5]. Wireless communications in optical window is called optical wireless communications (OWCs). OWCs utilize three different regions of the electromagnetic spectrum (EM), i.e., infrared (IR), visible light, and ultraviolet (UV). The optical spectrum window is illustrated in Fig. 1. Wireless infrared communication (WIRC) systems utilize the near-infrared (NIR) portion (IR-A) which occupies wavelengths from 780 nm to 1400 nm of the entire IR wavelength range $(780 – 10^6$ nm). IR-A extends from the nominal red edge of the visible spectrum. Originally, IR-A was targeted for short-range wireless communications. IR-B (1400 – 3000 nm) is used mainly for long distance communications either guided (optical fibre) or free space optical communications. While, IR-C portion $(3000 – 10^6$ nm), which is also called thermal imaging region, has been extensively used for military applications such as missiles homing and civilian purposes such as remote temperature sensing. Visible light communications (VLCs) use the entire visible light wavelength region (380 – 780 nm). Wireless ultraviolet communications (WUVCs) employ UV-C (200 – 280 nm, the deep UV) segment of the entire UV wavelength range (10 – 380 nm) [6], [7]. Furthermore, UV-A and UV-B are suitable for a wide range of applications including commercial, military, medicine, and dentistry applications [8]. The last part of the UV spectrum called extreme ultraviolet (EUV). This range of wavelengths is absorbed almost completely by the earth's atmosphere [9]. Therefore EUV requiring high vacuum for transmission.

Looking back into history, OWCs predate RF techniques by many centuries. Each nation had its own way of using fire signals to warn possible invasion or announce victory. About 800 BC, ancient Greeks and Romans used fire beacons in order to guide ships toward the mainland. In 1880, a light based telephone called photophone was innovated by Alexander Graham Bell to send and receive sound clearly over sunlight via unguided channel for a distance of some 213 m, and shorter ranges were covered using various lamps
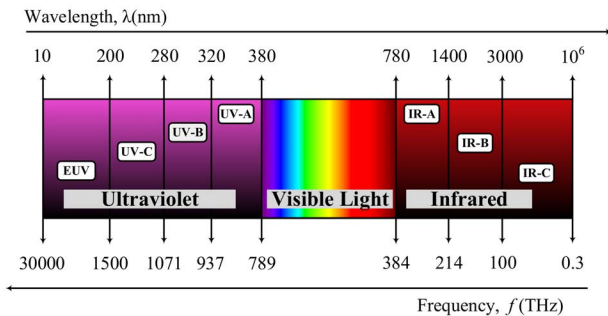
Fig. 1. The optical spectrum.

as a light source. Photophone was considered as the first VLC device [10]. For military purposes, German Army introduced IR photophones in 1935. The light source was a tungsten filament lamp combined with an IR transmitting filter. IR photophones succeeded in communicating over a range of 3 km at daylight and a clear weather [11]. In 1955, Rubin Braunstein, from the Radio Corporation of America (RCA), reported IR emission from a simple diode structured from gallium arsenide (GaAs). Two years later, in 1957, Braunstein further demonstrated that such a diode can be used for WIRCs through sending an audio signal to be detected by a lead sulfide (PbS) diode some distance away [12]. In 1962, Texas instruments (TI) manufactured the first commercial infrared light-emitting diode (IRED) product, which was structured from GaAs compound with emission in the 900 nm wavelength range [13]. By the fall of 1962, groups at IBM research laboratory, MIT Lincoln laboratory, and general electric (GE) succeeded in demonstrating IR laser diode (LD) [14]. During the same year, unlike others in RCA, Nick Holonyak chose gallium arsenide phosphide (GaAsP) alloy rather than off-the-shelf GaAs to produce first visible lasing and non-lasing light-emitting diode (LED). Holonyak is seen as the "father of the light-emitting diode" [13]. Thenceforth, advanced visible LEDs, which are capable of switching between different light intensity levels at a very fast rate, became available. The switching speed was fast enough to be imperceptible by human eyes. Consequently, a short VLC link of 5 m was first proposed in [15]. In VLCs, phosphor-based white-LEDs or red, green, blue LEDs (RGB LEDs) are used as a data transmitters, while a p-type/intrinsic/n-type (PIN) diode, avalanche photodiode (APD), or optical camera can be utilized as optical receivers.

On the other hand, studies on WUVC techniques date back to at least 1945 [7], mainly for long range communication based on UV-A sources such as carbon arcs, low pressure mercury arc lamps, gallium lamps, and nitrogen filled tubes. These devices are typically bulky, power hungry, or bandwidth limited [8], while receivers were, in most cases, photomultiplier tubes (PMTs) [16]. The first UV-A LED was reported by Jacques Pankove at RCA in 1972 using gallium nitride (GaN) alloy. Sensor Electronics Technology (SET) has developed a state-of-the-art miniaturized UV-C LEDs, called UVTOP series, in 2002 [17]. Since then, UV-C has the potential to be used in short-range wireless communication and sensing.

The very latest UV LEDs-based communication test-bed was reported in [18]. The setup can reliably deliver a data rate of 2.4 kbps for a vertically pointing transmitter and receiver of 11 m separation. Rapid development in compound semiconductor design and fabrication of LEDs, photodiodes (PDs), and filters, has inspired recent research and development in the OWC technology.

Since IR, visible light, and UV bands exhibit different optical properties, the propagation characteristics of the optical channel between the optical transmitter or source (OTx) and the optical receiver (ORx), are therefore different. Consequently, an accurate propagation channel model is indispensable to design an accurate and an efficient OWC system. In the literature, many survey papers have been published in terms of channel measurements and models in IR and UV bands, while very few in the visible light band. The previous work considered each band individually such as [7], [11], [19], and [20]–[22] or in a specific environment as in [23]–[25]. This motivates the need to present a comprehensive survey of optical wireless channel measurements and models that conducted in IR and visible light bands considering different environments, i.e., indoor, outdoor, underwater and underground.

The rest of the survey is organized as follows. Section II providing an overview of WIRCs, VLCs, and WUVCs technologies in terms of evolution and growth. In Section III, various scenarios of OWCs links are presented and the trade-off between their features is thoroughly explained. OWCs channels' characteristics have been detailed in Section IV. An overview of measurement campaigns and the state-of-the-art of indoor OWCs channel models are presented in Section V. Outdoor OWCs channel models and measurement efforts are introduced in Section VI. In Section VII, Underwater OWCs channel modeling approaches and measurement trials are given. While underground OWCs channel models and measurement campaigns are reviewed in Section VIII. The future research directions for conducting OWCs channel measurements and models are outlined in Section IX. Finally, concluding remarks are drawn in Section X.

II. OPTICAL WIRELESS COMMUNICATIONS (OWCS)

Shifting to higher frequencies towards optical frequencies reduces the wavelength of the electromagnetic waves. Therefore, the propagation loss through a specific environment is typically very high due to path loss (PL), which is proportional to $1/\lambda^2$ [26], and scattering (proportional to $1/\lambda^4$ in case of Rayleigh scattering) [27]. This limits the range of communication systems, but it makes OWCs attractive for a variety of short-range wireless communication applications [28]. Although there are some differentiations among IR, visible light, and UV characteristics, OWCs in general, utilize the intensity modulation (IM) scheme. This is due to the fact that the phase or frequency modulation of the incoherent waves is difficult [29]. On the other hand, direct detection (DD) is considered as the most practical down-conversion technique. Due to the reduced cost and complexity, IM/DD has been considered as the de-facto modulation scheme for OWCs [10].

OWCs suggest several notable features in terms of ecology, economy, and security when compared with RF communications. In this context, OWCs have no health concerns since optical frequencies are non-ionizing radiation. In terms of economy, OWCs are energy-efficient, low-cost [1], and offer higher area spectral efficiency (ASE), particularly in VLCs [30]. Last but not least, OWCs have inherent security due to spatial confinement of optical beams, taking into account that UV-C cannot even penetrate ordinary window glass [31]. In the following subsections, we highlight the most important research topics in the field of OWCs development in addition to present some engaging features for each optical window.

A. Wireless Infrared Communications (WIRCs)

As a complementary access technology to the RF techniques, a WIRC system was first proposed as a medium for short-range wireless communication more than three decades ago. IRED sources operating at 950 nm are used to establish an indoor optical wireless link of range up to 50 m [32]. Initially, several IR commercial products were available. IR devices from the same manufacturer could communicate with each other while competing manufacturers tended not to be interoperable. This necessitated, of course, establishment of a ubiquitous IR standard. Consequently, in 1993, the infrared data association (IrDA) had its first meeting. Accordingly, the first wireless infrared transmission standard promoted by a hundred of companies just one year and two days after the initial meeting [33]. IrDA suggests recommendations for short line-of-sight (LoS) links of range up to 1 m [34]. IrDA today permits tens of millions of users to easily beam data between handheld devices such as mobiles, laptops, and camcorders. According to IrDA, data can be exchanged through different protocols such as infrared mobile communications (IrMC), infrared communications (IrCOMM), and object exchange (OBEX) [35]. In 1999, IEEE 802.11 standard was released. Diffuse infrared physical layer (IR PHY) and medium-access control (MAC) layer technologies were specified in a specific clause. Unlike IrDA, the IR PHY is not directed and operates only in indoor environments. According to IEEE 802.11, different local area networks (LANs) using the IR PHY can operate in adjacent rooms separated only by a wall without interference, and no possibility of eavesdropping. IR PHY intended to allow for reliable operation at link lengths up to 10 m utilizing OTx of peak-power wavelength between 850 nm and 950 nm [34]. However, the mechanisms described in that clause are obsolete today [36]. In terms of safety, eye safety restrictions should be considered in WIRCs [37]. This is due the fact that IR-A rays can pass through the cornea and lens and focused on the retina. Therefore, intense IR-A exposure of the eye may cause retinal burns. Furthermore, since IR-B and IR-C can be absorbed by the cornea and lens, thermal injuries of the cornea and lens can occur after many years of exposure [38]. In terms of applicable environments, WIRCs have been applied in indoor, outdoor, and underground communication environments.

B. Visible Light Communications (VLCs)

Tech visionaries promised a bright future, in which, the fluorescent lamps and the wasteful little heaters incandescent light bulbs will be replaced with cool and efficient WLEDs. In the past decade or so, the implementation of LEDs lighting has been increased to a level where, in some parts of the world, incandescent bulbs have become obsolete [39]. Furthermore, more than a dozen countries have already enacted legislation that bans, or will soon ban incandescent bulbs [40]. The idea of illumination and data transmission simultaneously by using WLED was first proposed, for wireless home link (WHL), by a research group at Keio University in Japan [15]. In 2003, the visible light communications consortium (VLCC) was established by Nakagawa Laboratories in partnership with CASIO, NEC, and Toshiba in Japan [41]. VLC technology became sufficiently mature to be standardized by IEEE 802.17.5 working group, in 2011 [42]. IEEE 802.17.5 included the link layer and physical layer design specifications. Based on VLC idea, light fidelity (Li-Fi) term is coined by Harald Haas [6]. Li-Fi providing bi-directional VLC system by utilizing IR or Wi-Fi for uplink. For instance, the first generation, commercially available full duplex Li-Fi modem using IR for the uplink channel was announced by pureLiFi [43]. OLEDCOMM was the first European company that starts to commercialize Li-Fi communication solutions a worldwide level [44]. Most recently, IEEE 802.15.7 task group announced a call for proposals (CFP) for the development of the IEEE 802.15.7 r1 standard to be revealed by the end of 2017 [45]. IEEE 802.15.7r1 technical consideration document aims to provide three main sections including optical camera communication (OCC), Li-Fi, and LED-identification (LED-ID). OCC is a VLC system but combined with a camera. OCC provide triple functions, i.e., illumination, data transmission/receiving, and positioning/localization.

Unlike WIRCs and WUVCs, VLCs possess the ability to provide illumination and wireless broadband communication simultaneously. Hence, WLEDs lighting features, compared with the conventional lighting technologies, i.e., incandescent and fluorescent bulbs, should be considered. WLEDs have high luminous efficiency (consumed electricity to provide the intended illumination) of 107 lumens/watt (LED T8 Tube) [46] compared to 15 lumens/watt and 60 lumens/watt for incandescent and fluorescent bulbs, respectively [21]. Similarly, WLEDs have a long lifespan of 50000 hours compared to 1200 hours and 10000 for incandescent and fluorescent bulbs, respectively. Furthermore, LEDs (or Organic LEDs (OLEDs) for future VLCs) are environmental friendly, without Mercury or any other hazardous substances and with low heat radiation in case of long period of continuous usage. However, intense visible light exposure can lead to thermal retinal injuries. Therefore, illumination must comply with the lighting standards to ensure eye safety and avoid light flicker. For instance, illuminance span of 300 – 1500 lux is required for typical office work [47]. VLCs can be applied in indoor, outdoor, underwater, and underground communication environments.

C. Wireless Ultraviolet Communications (WUVCs)

Within the entire UV spectrum, the UV-C band exhibits unique properties present the opportunity to overcome some specific OWCs challenges. UV-C band is solar blind, which means that UV-C in the solar radiation has been mostly absorbed by ozone in the upper atmosphere [48]. Therefore, employing a wide field-of-view (FoV) ORx, the WUVC systems will encounter virtually noiseless communication channel, and hence achieve excellent signal-to-noise ratio (SNR) [49]. That is not the case, for example, with WIRCs and VLCs because of the non-negligible ambient light interference due to background solar radiation. Furthermore, UV light is strongly scattered by molecules, aerosols, haze, fog, and other particles in the atmosphere because of the short wave-length (Rayleigh scattering). This is, however, can be exploited to relax or eliminate the acquisition, pointing, and tracking (APT) requirements. Consequently, a non-directed non-line-of-sight (NDNLoS) WUVC link can be established easily when the directed LoS (DLoS) link is vulnerable to being blocked. This is due that some of the transmitted light, which is scattered in the direction of the ORx, will be detected and a communication channel will be established [50]. In case of DLoS link, when the communication range increases or visibility decreases (high aerosol concentration), forward scattering may significantly affect link performance. While, decreased visible range may result in enhanced NDNLoS link [8]. Therefore, most of WUVC applications relay on NDNLoS links. This mechanism is, however, the opposite of that in conventional WIRCs and VLCs channels. In terms of safety, WUVCs applications must be tempered by eye and skin exposure limits. In this context, UV-A rays can be absorbed by eye lens and hence can cause cataracts. While UV-B and UV-C rays are absorbed by the cornea and may damage the corneal tissue. On the other hand, UV radiation is believed to cause long-term effects such as skin aging and skin cancer [38]. Finally, it is worth to mention that although the WUVCs have existed for decades, the realization of compact, low-power systems has only recently begun to materialize and therefore, a variety of potential applications and research topics remain open [7]. WUVCs have been applied in indoor, outdoor, and underwater communication environments [51].

III. OWC CHANNEL SCENARIOS

The characteristics of the optical wireless channel can vary significantly depending on the optical wireless channel scenario (also called link configuration, link design or topology in many literature). This section presents the most common optical wireless link designs, while their specifications and the trade-off between them have been explained in the following subsections. In principle, all communication technologies within OWCs share common link designs. However, some link designs are only applicable for specific scenarios and such examples will be presented. Basically, it is convenient to classify OWC link configurations according to three criteria. Firstly, the degree of directionality of the OTx and ORx. Secondly, the existence of uninterrupted LoS path between the OTx and ORx. Thirdly, the OTx divergence angle and the FoV
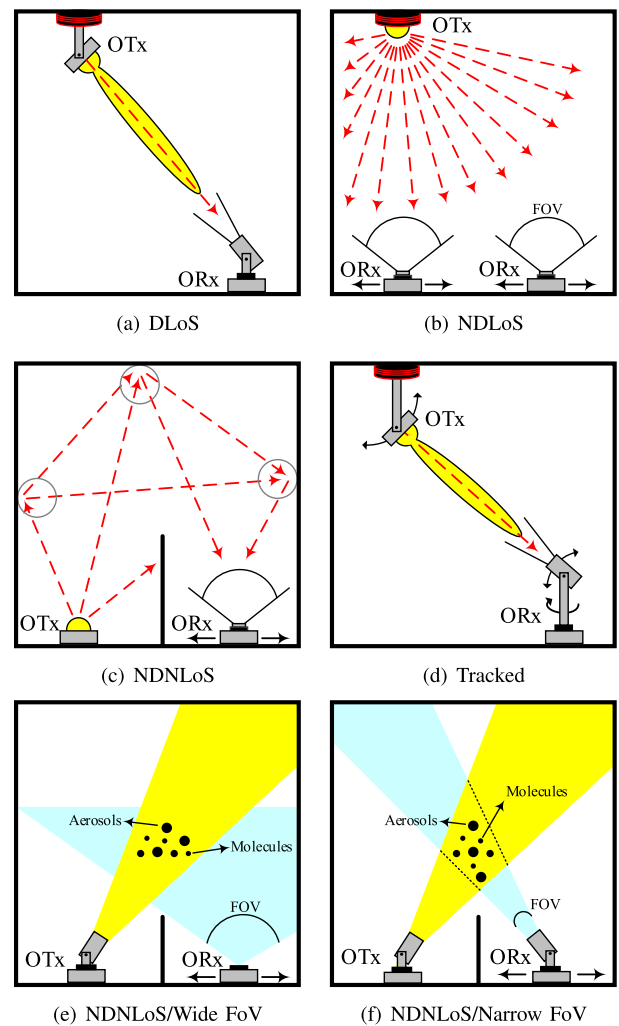

Fig. 2.   OWC channel scenarios.

of the ORx. Accordingly, there are four common link configurations mostly referred in literature as 1) DLoS; 2) Non-Directed LoS (NDLoS); 3) NDNLoS; and 4) Tracked [8], [10], [52], [53]. Aforementioned link configuration classifications are illustrated in Fig. 2.

1) DLoS: This design is shown in Fig. 2(a). It is practicable in all OWCs technologies, especially in WIRCs. DLoS is also applicable in all above environments. It is established when the OTx is oriented towards the ORx. This design is utilized in point-to-point (P2P) and simple peer-to-peer networking OWC links [54]. It is commonly used for indoor short-range communications. Whereas, for outdoor communications, lasers rather than LEDs are being employed in most cases, e.g., free space optical networking architecture (FSONA) technology which utilizes IR-B band [55]. DLoS design offers low power requirement (maximizes power efficiency) because the optical channel loss will be limited only by free space PL and hence higher data rate can be obtained. This is, however, at the cost of limited mobility, small coverage area, and stringent link alignment [96]. The main drawback of DLoS link is sensitive to blockage and shadowing [53].

2) NDLoS: Sometimes called wide LoS (WLoS) [57]. This link is most suitable for point to multipoint indoor communication applications. As seen in Fig. 2(b), this design exhibits more flexibility since both OTx and ORx have wide optical aperture, i.e., wide beam divergence angle for the OTx and wide FoV for the ORx. Accordingly, no alignment is necessary and therefore, NDLoS links may be more convenient to use, particularly for mobile terminals since they do not require orientation of the OTx or the ORx [53]. Furthermore, due to reflections from roomâĂŹs walls, objects and fixtures, this link configuration shows more robustness to shadowing and blockage. On the other hand, reflections are considered the main reason for increasing the PL in addition to multipath dispersion which ultimately leads to the transmission bandwidth limitation [96]. NDLoS links are applicable in all OWCs technologies, particularly in VLCs, since it provides illumination in the first place. This scenario is most applicable in indoor and underground communication environments.

3) NDNLoS: This link design does not impose LoS connection between the OTx and ORx. This design is well known as diffuse link configuration in WIRCs. In this configuration, an OTx with wide beam divergence is pointed towards the ceiling. The diffuse reflections off ceiling, walls, and objects are used to establish a link to a wide FoV ORx that also faces the ceiling as shown in Fig. 2(c). Diffuse link maintains sustained connection between the OTx and ORx. Consequently, this will offer users a wide degree of mobility and high robustness against link loss due to blockage [58]. Since no LoS required, the diffuse configuration is considered the most convenient for both infrastructure and ad hoc networks. Unfortunately, diffuse configuration sustains high PL due to the absence of a direct path, typically 50-70 dB for a horizontal separation of 5 m in WIRCs [10]. In addition to high PL, diffuse configuration experiences multipath dispersion. Multipath dispersion induced intersymbol interference (ISI) and consequently bit error rate (BER) degradation and hence limiting data rate [59]. Multipath power penalty is added in order to overcome ISI, therefore this link configuration is less power efficient than aforementioned links. Furthermore, NDNLoS link configuration is commonly used in WUVCs, but it is based on scattering from the particles in the atmosphere rather than diffuse reflection in WIRCs as illustrated in Fig. 2(e) and Fig. 2(f). Based on a specific application, the ORx can be of wide or narrow FoV. Unlike diffuse WIRC link, the distance between the OTx and ORx in case of WUVC links is further. NDNLoS link configurations are more viable in WIRCs and WUVCs than in VLCs [60]. This link scenario is more relevant to indoor WIRCs and outdoor WUVCs.

4) Tracked: This scenario is illustrated in Fig. 2(d). It is proposed to enable user mobility, improve power efficiency, reduce multipath induced ISI, and provide high data rate within one link configuration [61]. A tracked system could be incorporated in either a ceiling-mounted transceiver (base station) or in a mobile terminal or both [62]. Tracking mechanism is done through three main components: an acquisition unit to observe the presence of a new mobile station within a specific area, a tracking unit to track this new mobile station, and pointing unit to aim the optical beam so that it is on or closely parallel to the required optical path (with tolerable offset). This technique is known as APT. Tracked configuration is more feasible in indoor WIRCs. However, mechanically steerable optics are expensive and difficult to miniaturize. Consequently, a solid-state tracking system that eliminates steering requirements was proposed in [62].

As a summary with the help of Section II and III, we can briefly show the key differences between WIRCs, VLCs, and WUVCs technologies as detailed in Table I. Here, RF communication technology has been added to the comparison in order to enrich this survey.

IV. OWC CHANNEL CHARACTERISTICS

It is worthwhile to emphasize that OWC link impairments can have a significant impact on system performance and capacity. Such impairments include the distortion, which is introduced by the optical wireless channel into the received signal. Therefore, in order to design, implement and operate an efficient OWC system, it is essential that the characteristics of the optical wireless channel are well understood so as to analyze and combat the effects of channel distortions. Channel characteristics of OWCs depend in the first place upon the type of communication environment, e.g., indoor, outdoor, underground, or underwater. Furthermore, environment details are affecting channel characteristics. For instance, indoor environments include household or office buildings, factories, shopping malls, etc., and these are extremely varied. Hence, different environment would cause different optical channel characteristics. Secondly, the positions and the mutual orientation of the OTx and ORx, as well as their orientation towards the reflecting surfaces. Therefore, applying indoor characterization techniques is not really effective for determining the outdoor (or underground and underwater) channel characteristics and system performance. Table II presents the most common communications environments and some of their examples.

Unlike RF channels, optical wireless channels do not experience multipath fading [10]. This is a result of, in OWCs, the PD dimensions are in the order of millions of optical wavelengths, which leads to an efficient spatial diversity that exhibits a high degree of immunity to multipath fading [10], [59], [65]. Therefore, there is no small-scale fading in OWCs. Furthermore, the use of IM/DD in OWCs systems eliminates the transmitter and receiver local oscillators and hence no frequency offset (FO) in OWCs. While in terms of Doppler shift, it has been shown in [66] that Doppler frequency has negligible effects in OWCs systems. This is because the corresponding wavelength shift is small enough to assume that bandwidth spreading and SNR variation due to Doppler are insignificant problems in most IM/DD systems. Although OWCs do not experience multipath fading, they do suffer from the effects of multipath dispersion, which manifests itself in a practical sense as ISI. In the following subsections, we will present a brief explanation of the primary characteristics of the optical wireless channels.

TABLE I
FEATURES OF WIRCs, VLCs, WUVCs, AND RF COMMUNICATIONS

	WIRCs	VLCs	WUVCs	RF Communications
Transmitter	IRED, IR Laser	Phosphor-based WLED, RGB LED	UVTOP LED	Typical Tx RF Antenna
Receiver	PIN, APD	PIN, APD, SPAD	UVPMT, DUVAP Combined with a solar blind filter	Typical Rx RF Antenna
Standard	IrDA (P2P), IEEE 802.11 (Diffuse)	IEEE 802.15.7 r1 (In progress)	N/A	IEEE 802.11x
Communication scenario	Mainly Indoor, secondarily outdoor	Mainly Indoor, secondarily outdoor and underwater	Mainly outdoor, secondarily underwater [7]	Indoor and outdoor
Link configuration	Mainly NDNLoS, secondarily DLoS	Mainly NDLoS	Mainly NDNLoS	NDLoS and NDNLoS
Dominant noise at the Rx	Background light	Background light	Virtually noiseless [7]	Interference noise
Multipath fading	No	No [10]	No	Yes [10]
Doppler effect	No	No	No	Yes
Path loss	High	High	Higher than WIRCs, VLCs and RF	High
Bandwidth	100 THz $-$ 384 THz, (IR-A & IR-B)	384 THz $-$ 789 THz	1071 THz $-$ 1500 THz (UV-C)	3 Hz $-$ 300 GHz
Bandwidth regulated	No	No	No	Yes
Cost	Low [37]	Low [1]	Low (based LEDs [7]) High (based lasers & flash lamps [49])	High [10]
Range	Short-range (indoor based IRED [32]), Long-range (outdoor based IR Laser) [55]	Short-range (indoor) Moderate-range (outdoor VVLC up to 100 m [63])	Long-range if compared with WIRCs and VLCs [8]	Short-range and long-range [1]
Communication mode	Mainly unidirectional	Mainly unidirectional	Bidirectional	Bidirectional
Power consumption	Low	Low	Higher than VLCs and WIRCs [8]	High [6]
Eye & skin safety	Potential eye hazard [37]	Potential eye hazard	Potential eye & skin hazards [38]	No obvious hazard
Penetration	Penetrate through glass but not walls, and opaque objects	Same as WIRCs	Do not penetrate through glass walls, and opaque objects	Penetrate through glass walls, and opaque objects

WLED: white-light-emitting diode; RGB LED: red, green, blue LED; PIN: p-type/intrinsic/n-type diode; APD: avalanche photodiode; SPAD: single photon avalanche diode; UVPMT: UV photomultiplier tube; DUVAP: deep ultraviolet avalanche photodetector; VVLC: Vehicular VLC; N/A: not applicable

A. Channel Impulse Response (CIR) h(t)

The optical wireless channel can be modeled as a linear time-invariant (LTI) system with input intensity $x(t)$, output current $y(t)$, and an impulse response $h(t)$, which is fixed for a certain physical design for the OTx, ORx, and reflectors [67]. CIR $h(t)$ is the time evolution of the signal received by the ORx when an infinitely short optical pulse is sent from the OTx [68]. CIR $h(t)$ allows predicting what the system's output will look like in the time domain. Once the CIR $h(t)$ is known, any waveform distortion due to multipath propagation can be calculated and the output of the system can be predicted for any arbitrary input without even testing it (when the system is LTI). Mathematically, the equivalent baseband model of an IM/DD optical wireless link can be expressed as [10]

$$y(t) = R_\lambda \ x(t) \circledast h(t) + n(t). \tag{1}$$

Here, the symbol $\circledast$ denotes convolution and $n(t)$ is the background light noise, which is modeled as a signal-independent additive white Gaussian noise (AWGN). Hence, characterization of the OWCs channels is performed by their CIR $h(t)$, which is used to analyze and combat the effects of channel distortions [10], [69]. Therefore, the starting point for capturing OWCs channel characteristics is to propose an accurate channel model and determine its CIR $h(t)$.

B. Channel DC Gain H(0)

For intensity-in intensity-out channels, the zero-frequency (DC) value of their frequency responses can be expressed as [52]

$$H(0) = \int_{-\infty}^{\infty} h(t)dt. \tag{2}$$

The expression in equation (2) is commonly referred to as channel DC gain, which is the fraction of power emitted from a continuous-wave transmitter that is detected by the receiver. Channel DC gain $H(0)$ is related to the average received power P_r, by $P_r = P_t \ H(0)$, where P_t is the average transmitted power. Furthermore, for on-off-keying (OOK) non-return-to-zero (NRZ) intensity modulation and encoding technique system, the signal-to-noise ratio (SNR) in dB is proportional to the square of the channel DC gain $H(0)$ as [10]

$$\text{SNR} = \frac{R^2 H^2(0) P_r^2}{R_b N_0}. \tag{3}$$

TABLE II
ENVIRONMENTS OF OWCS

Environment	Field of Application
Small-scale indoor	Typical rooms
Mid-scale indoor	Offices, labs, workshops
Large-scale indoor	Factories, sport complexes, shopping malls, hospitals
Open indoor	Train stations, airports, museums, exhibit halls
Intra-Vehicle	Vehicles, trains, airplanes
Inter-Vehicle/ Outdoor	Vehicle-to-vehicle (V2V), vehicle-to-road infrastructure (V2R), road infrastructure-to-vehicle (R2V), Point-to-point (P2P) [55]
Underground	Subway stations, underground roads and mines [64]
Underwater	Autonomous underwater vehicles (AUV), divers, underwater robots and sensors [7]

Here, R, N_0, R_b denote responsivity of the PD (A/W), the noise spectral density (W/Hz), and achievable bit rate (bps), respectively. Equation (3) clearly indicates that the SNR in OWCs systems is proportional to P_r^2 compared with P_r in the conventional RF channels. Consequently, this necessitates the need for higher optical power requirement and a limited path loss to deliver the same performance. Therefore, OWC technology, particularly VLC is considered as a good candidate for future short range communications.

C. Root Mean Square (RMS) Delay Spread

In NDLoS and NDNLoS link configurations, the optical signal takes multipath to reach a fixed or mobile ORx. Multipath propagation occurs due to reflections off surrounding environments. Due to the differences in propagation path lengths, the received signal appears as a sum of weighted, delayed copies of the transmitted signal [69]. Hence, the optical channel stretches the transmitted signal in time resulting in the so-called temporal dispersion. This major characteristic can be quantified by the RMS delay spread $D_{\rm rms}$ of CIR $h(t)$ as [70]

$$D_{\rm rms} = \sqrt{\frac{\int_{-\infty}^{\infty}(t-\mu_\tau)^2\ h^2(t)dt}{\int_{-\infty}^{\infty}h^2(t)dt}}. \tag{4}$$

Here, t is the propagation time and μ_τ is the mean excess delay given by [70]

$$\mu_\tau = \frac{\int_{-\infty}^{\infty}t\ h^2(t)dt}{\int_{-\infty}^{\infty}h^2(t)dt}. \tag{5}$$

Equation (4) indicates that different environments and OTx-ORx configurations can significantly affect $D_{\rm rms}$, and smaller values of $D_{\rm rms}$ indicate a higher system transmission bandwidth. Based on $D_{\rm rms}$, channel coherence bandwidth can be expressed as [71]

$$B_{\rm c,50\%} = 1/(5D_{\rm rms}). \tag{6}$$

Here, 50% denotes the decorrelation percentage. It is worth mentioning that although OWCs channels do not experience multipath fading, if the LED modulation bandwidth exceeds the channel coherence bandwidth, the channel can be characterized as a frequency selective channel due to dispersion [71]. Likewise, based on $D_{\rm rms}$, the maximum bit rate R_b which can be transmitted through the optical wireless channel, can be expressed as [72]

$$R_b \leq 1/10D_{\rm rms}. \tag{7}$$

It should be noticed that at long transmission distances, there will be a noticeable difference between the optical path delays. Therefore, we may be concerned with ISI for higher transmission data rates.

D. Frequency Response $H(f)$

The impact of multipath effect on the optical wireless channel bandwidth can be easily seen in frequency domain rather than time domain. Channel frequency response $H(f)$ can be estimated by using Fourier transform of CIR $h(t)$. The 3-dB frequency of the optical channel can be obtained as [73] and [74]

$$|H(f_{\rm 3dB})|^2 = 0.5|H(0)|^2. \tag{8}$$

It has been proved that the higher-order reflections have significant impact only at low frequencies whereas the high-frequency magnitude response is characterized by the first-order reflection [75]. Furthermore, it has been shown that the variation of the received power in environments with different reflectivity and the available bandwidth are almost inverse to each other [6]. Miramirkhani *et al.* [76] have shown that most materials have a higher reflectance in IR spectrum rather than in visible light spectrum. Highly reflective geometry encounters low path loss and hence high power will be received from different propagation paths, resulting in high delay spread and low channel bandwidth. Consequently, VLCs provide a larger transmission bandwidth compared with WIRCs.

E. Optical Path Loss (PL)

Although OWCs do not experience small-scale fading, large-scale fading due to PL and shadowing considers as primary characteristics for the optical wireless channels. In DLoS and tracked channel scenarios, indirect propagation paths contribution can be neglected. Thus, unshadowed LoS PL model is expressed based on the knowledge of the radiated pattern, ORx size and the square of the distance between the OTx and ORx [10], [59]. However, in the NDLoS and NDNLoS channel scenarios, the prediction of the optical PL is more complex since it depends on environment parameters such as reflectivity, absorption, scattering, orientation and position of the OTx and ORx. The PL of unshadowed diffuse configurations can be estimated using the expression [59], [77]

$$\mathrm{PL_{Diffuse}}\ (\mathrm{optical\ dB}) = -10\log_{10}\left(\int_{-\infty}^{\infty}h(t)\ dt\right). \tag{9}$$

Therefore, to estimate the optical PL, it is necessary to analyze the CIR $h(t)$ for a given environment. There are different

attempts to accurately estimate the optical PL in different environments and scenarios. For instance, Dimitrov *et al.* [83] have developed PL models for WIRCs inside an intra-vehicle environment, i.e., aircraft cabin. An indoor VLC PL model for a mobile user has been proposed in [77]. Moreover, a PL model for VLCs in an underground mining environment is proposed in [79].

F. Optical Shadowing

Channel PL is increased further if a temporary obstruction, such as a person or an object obscures the ORx such that the main signal path is blocked or partially obstructed. This situation is referred to as optical shadowing, which is another vital factor that affects the performance of OWCs systems. Unlike RF waves, optical waves cast clear shadows (hard shadow). This is due to the fact that the optical waves have very short wavelengths compared to the size of the obstacles, and hence they do not diffract noticeably [80]. For indoor environments, it has been shown that signal path obstruction by furniture can be easier predicted and hence avoided through the implementation of the appropriate channel scenario and OTx/ORx orientation. However, the obstruction caused by the random movement in indoor and other environments makes optical channel vulnerable to shadowing and hence greatly affects the received signal strength. For example, for indoor WIRCs, shadowed NDLoS and diffuse channels have been investigated in [81] and [82]. For intra-vehicle WIRCs, Dimitrov *et al.* [83] adopted the already existing RF PL model that including shadowing to WIRCs. Consequently, optical PL exponent and shadowing standard deviation values have been estimated for different propagation paths and scenarios inside an aircraft. It is worth mentioning that the previous studies were based on using curve-fitting methods based on experimental data. In terms of indoor VLCs, the most studies primarily focus on the modeling and analyzing the shadowing and blockage that caused by moving or stationary people [80], [84].

V. INDOOR OWCs CHANNEL MEASUREMENTS AND MODELS

A. Channel Measurements

This section presents a brief survey of the conducted measurement campaigns of OWCs, mainly for WIRCs and VLCs. However, a complete survey of WUVCs channel measurements and models is beyond the scope of this paper. This is due to the fact that WUVC channels exhibits different propagation characteristics due to molecular and aerosol scattering. For instance, in the case of DLoS channels, the multiple scattering is more pronounced than in an NDNLoS channels. Furthermore, decreased visibility range may result in enhanced NDNLoS channels, the opposite of conventional optical channels [8]. Therefore, WUVCs are mainly NDNLoS. Here, the authors would like to draw the reader's attention to the fact that there has been a long history of research on WUVCs channel measurements and modeling reported in the literature that can be found in [7], [8], [16], [48], [60], and [85].

There is also a rich history of relevant studies on measurement based WIRC channel modeling conducted since the 1990s, e.g., [59], [75], and [86]–[91]. In order to understand the underlying physical phenomenon of optical wireless signal propagation in indoor environments and validate the proposed optical channel propagation model, measurement campaigns need to be carried out. A perfect channel model is a model, that perfectly fits against the measured channel [69]. Therefore, some proposed channel models were combined with experimental measurements to verify the proposed channel model, e.g., [75] and [86]. On the other hand, some channel models have been verified based on the measurement campaign of the others, such as in [87]. As a side note, in order to avoid the repetition, channel models that associated with validation measurements will be listed in next subsection.

Barry *et al.* [75] presented a recursive optical wireless channel model which is verified by measurements. Power measurements have been conducted using Si APD and a transimpedance amplifier (TIA). While, the frequency response of the channel, measured using a 300 kHz – 3 GHz vector network analyzer. Although Barry's recursive model has been verified by measurements, that model was applicable only to particular room environments and scenarios, which are detailed in [75]. Consequently, Barry *et al*. could not make general statements about all room configurations. Since the early experimental measurements of WIRC channels that done by Barry *et al*. [75], many other research groups have begun to investigate more WIRC channels' characteristics. Based on measurements results, Hashemi *et al.* [88] have reported that indoor WIRC channels are very dynamic with significant variations in the channels' characteristics. These results were based on the data that collected from various rooms for different ORx locations within the same room, in addition to considering different orientations of the ORx for each location. The authors utilized a network analyzer to modulate the intensity of NIR LD which is directed on a flat piece of cardboard painted white to ensure diffuse reflection to be detected by a PD. The research work on measurements and modeling of indoor RF channels in [92] has been extended by the same working group to consider diffuse indoor WIRCs. The results of the analysis emphasize that WIRCs are a suitable candidate for high speed wireless data communication inside buildings. In [59], more generalized measurements based research on approximately 100 different WIRC channels. Both NDLoS and diffuse link configurations have been considered, with and without shadowing. The experimental work based on the same types of equipment as in [88], but an APD is used. The study pointed out that the unshadowed NDLoS configurations generally have smaller optical PL, D_{rms}, and power penalties compared with their unshadowed diffuse counterparts. On the other hand, shadowed NDLoS configurations, generally exhibit larger values of the above three characteristics compared with the corresponding shadowed diffuse configurations. Another measurement campaign is reported in [90] to examine the WIRC channels' characteristics and system performance. The measurements were conducted in the absence of ambient light and under different lighting conditions to quantify the impact of ambient light noise. The measurement setup consisted of a hemispherical concentrator with a hemispherical bandpass optical filter attached to a PIN PD. Furthermore, a

high-impedance hybrid preamplifier and high-pass filter have been used to achieve a high SNR and mitigate fluorescent light noise, respectively.

Measurement-based stochastic approach in WIRCs was first introduced in [91] to compute the diffuse CIR $h(t)$ of indoor WIRCs. Compared with iterative method in [52], stochastic approach offers increased flexibility and reduced computational complexity. The authors have utilized about 14000 measures of CIR $h(t)$ to fit the shape of certain well-known distributions, i.e., Rayleigh and Gamma. The fitting process was carried out using Cramér-von Mises (CvM) and minimum square error (MSE) criteria. The study, however, has not considered the presence of the LoS components. Based on their previous work in [88], the same working group have performed further comprehensive measurements campaign to investigate the impacts of receiver rotation and shadowing on the indoor WIRC channels. The measurements have been executed in nine different rooms in the Colonel By Hall (CBY) at the University of Ottawa [81]. The study adopted both NDLoS and diffuse link configurations. The measurements results have presented several outcomes that are helpful in the characterization of WIRC channels. It has been observed that the variations of optical wireless channel PL for small changes of ORx rotation in NDLoS channels, is well approximated by a Gamma distribution. The results have also demonstrated a correlation between the channel D_{rms} and channel PL for both NDLoS and diffuse link configurations. Consequently, a simple formula has been provided to express that correlation. Furthermore, measurements have also been proved that shadowing reduces the received optical power and increases the channel D_{rms}. Jungnickel *et al.* [61], have conducted measurement campaigns to verify the spherical channel model for WIRCs. Both tracked and diffuse configurations have been considered. The received power of modulated NIR LD light detected by an APD, and the frequency response measured using S-parameter test set network analyzer. Likewise, in [86], HAYASAKA-ITO channel model, has been verified by channel measurements which are carried out by using an APD and the frequency sweep method. More details regarding the outcomes of previous two models will be given in next section.

On the other hand, in terms of VLC channel measurements, it has been noticed that there is a few measurement campaigns have been conducted for the indoor VLC channels and they are mostly confined to NDLoS link configuration. An early straightforward experimental work for VLC channel measurements was performed by Samsung Electronics [93]. The received light is measured by a PIN PD and the data is sampled by an oscilloscope and analyzed using MATLAB. Cui *et al.* [94], have derived the PL in the photometric domain for short range NDLoS channel. The experiment setup consisted of a commercial PD with an internal TIA. A concentrator is attached to the PD along with an optical bandpass filter. The output of the PD is fed to a laptop through a RS232 cable and the corresponding interface. In [74], VLC channel measurements were carried out in a rectangular empty dark room. PMT with TIA is used to detect the diffused optical signal. Furthermore, frequency response has been investigated experimentally using both the short pulse and the frequency

sweep techniques. In the later study, for the comparison purpose, the iterative site-based modeling technique [95] was adopted for the CIR $h(t)$ simulation of the indoor VLCs. Despite the impact of higher-order reflections consideration in measurements, the results showed a good agreement between simulation and measurements. Another measurements campaign is conducted in [96] in order to investigate diffuse indoor VLC channel's characteristics. It has been demonstrated that the coverage area in indoor VLC systems can be increased by using holographic light shape diffuser (LSD) with suitable angles. In terms of shadowing, Xiang *et al.* [80] have considered the effect of channel PL and shadowing. Two persons of different height and weight have been used as a temporary obstruction to model the shadowing in VLCs. The measurements have been carried out with a spectrum analyzer, an arbitrary waveform generator (AWG), and a PMT, where all ambient lights were turned off to eliminate interference. In [97], the effect of people movement on indoor VLC channel's characteristics, such as received power and D_{rms}, was investigated in three indoor scenarios, i.e., a furniture equipped office room, an empty hall, and a corridor. The received power was measured using the Thorlabs digital power meter, and three irregular shapes of the obstacles have been randomly placed to represent people existence. Measurement results showed that VLC technology is robust enough for indoor communications since it is offering excellent mobility even when considering an environment with high people density. In [98], an indoor visible light positioning system is proposed. An experimental demonstration has been carried out to verify the feasibility of indoor positioning, LED identification (LED-ID) scheme inside a laboratory. LED lamps that are driven by the microcontroller unit (MCU) and Pad platform, which is consist of the PD module and an Android Pad device have been used. Another VLC positioning system based OFDM access (OFDMA) has been reported in [99].

In this study, we have listed (in chronological order) the important measurements campaigns for WIRC and VLC channels according to the publishing year, environment, scenario, measured channel characteristics, and the operating wavelength as detailed in Table III.

B. Channel Models

In terms of channel modeling approaches, there are many channel models for conventional WIRCs reported in [32], [61], [75], [83], and [100]–[105]. On the other hand, in terms of VLC channel modeling, an explicit state-of-the-art of VLC channel models has not been investigated adequately yet. Although few literary works related to VLC channel modeling have been reported in [77] and [106]–[111], research in this area is still at an early stage. Furthermore, the IEEE 802.17.5 does not specify VLC channel models to be used for technology evaluation yet [110]. Therefore, an explicit generic channel model that can be adapted to a wide range of VLC scenarios is still missing in the literature. In order to summarize what has been done so far in the literature, the most important indoor OWC channel models, mainly for WIRCs and VLCs,

TABLE III
IMPORTANT OWCs CHANNEL MEASUREMENT CAMPAIGNS

Ref.	Year	Environment	Scenario	Channel Characteristics	Operating Wavelength
[88], [89]	1994	8 Different furnished rooms at the uOttawa	NDLoS and diffuse	$H(f)$, PL	NIR LD (λ= 810 nm)
[59]	1995	5 Different rooms: 2 empty, and 3 furnished rooms	NDLoS and diffuse	$h(t)$, $H(f)$, D_{rms} PL, Shadowing	NIR LD (λ= 832 nm)
[90]	1996	4 Different empty rooms	NDLoS and diffuse	$h(t)$, $H(f)$, D_{rms}, PL	NIR LD (λ= 806 nm)
[91]	1997	Empty square room	Diffuse	$h(t)$, D_{rms}, μ_τ	NIR IRED (λ= 832 nm)
[81]	2001	9 Different furnished rooms at the uOttawa	NDLoS and diffuse	$h(t)$, $H(f)$, D_{rms}, PL	NIR LD (λ= 808 nm)
[93]	2008	Rectangular furnished room	NDLoS	$h(t)$,	Red LED (λ= 650 nm)
[94]	2010	Rectangular empty room	NDLoS	$H(0)$, PL	White LED (λ= 380−780 nm)
[96]	2012	Rectangular empty room	NDLoS	$H(0)$	Blue LED (λ= 455 nm)
[74]	2012	Rectangular empty dark room	Diffuse	$h(t)$, $H(f)$	Blue LD (λ= 445 nm)
[80]	2014	Furnished meeting room	NDLoS and diffuse	$h(t)$, D_{rms}, μ_τ PL, Shadowing	White LED (λ= 380−780 nm)
[97]	2015	Corridor, empty hall furnished office room	NDLoS	$H(0)$, D_{rms}, μ_τ	White LED (λ= 380−780 nm)
[98]	2017	Laboratory	NDLoS	$h(t)$, $H(0)$	White LED (λ= 380−780 nm)
[99]	2017	Large hall	NDLoS	$h(t)$, $H(0)$	White LED (λ= 380−780 nm)

NDLoS: Non-directed LoS; $h(t)$: channel impulse response; $H(f)$: channel frequency response; PL: path loss; D_{rms}: root mean square delay spread; μ_τ: mean excess delay; NIR: near-infrared; LD: laser diode; LED: light-emitting diodes; IRED: infrared light-emitting diode; uOttawa: University of Ottawa; N/A: not applicable

are presented in Table IV. As can be seen, the OWC channel models are briefly reviewed and tabled according to the year of publishing, modeling approach, environment, scenario, investigated channel's characteristics based on each approach, the number of bounces, and the operating wavelength.

The OWC channel models that are presented in Table IV can be classified as deterministic and stochastic models. For instance, different approaches are included in the deterministic approach, e.g., recursive [75], iterative [95], DUSTIN [87], geometry-based deterministic models (GBDMs) based on ray-tracing [106]–[108], and ceiling-bounce model (CBM) [67]. On the other hand, the stochastic models can be further classified into geometry-based stochastic models (GBSMs) and non-GBSMs. Models such as spherical model [61] and regular-shaped GBSM (RS-GBSM) [111] can be classified as GBSMs. While, models such as Monte Carlo algorithm (MCA) [100], and modified CBM (MCBM) [112] are classified as non-GBSMs. MCBM uses a combination of the traditional CBM and a stochastic approach in order to mitigate the computational complexity of deterministic models. Fig. 3 illustrates OWCs channel models classification for most common channels models. Here, we have highlighted some of OWCs channel models with related literature, while in the following subsections, we will give a descriptive overview of each channel model individually.

1) Deterministic Channel Models: Deterministic channel models are usually based on the detailed description of specific propagation environment, channel scenario, and the position and orientation of the OTx and ORx. The CIR $h(t)$ of the OWC system is obtained using intensive simulations that incorporate details of propagation environments like rooms, offices,
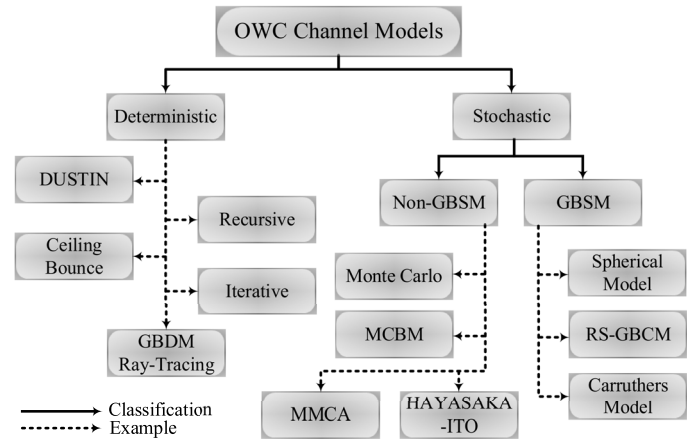

Fig. 3. OWC Channel Models.

buildings, roads, etc. Therefore, these models are site specific, physically meaningful and potentially accurate. Below is a brief review of various approaches of deterministic channel models for OWCs.

a) Recursive Model: This model was presented by Carruthers [34], Kahn and Barry [53], and Barry *et al.* [75]. The recursive approach is advised primarily to evaluate the CIR $h(t)$ of multiple-bounce (more than two reflections) in WIRCs. It has been considered as an extension of the single reflection cavity model which proposed by Gfeller and Babst in [32]. Here, much interest has been given to recursive approach comparing with cavity model since it is more comprehensive in terms of WIRCs channel modeling. In this model, the radiation intensity pattern $R(\phi)$ for a particular

TABLE IV
IMPORTANT OWCs CHANNEL MODELS

Ref.	Year	Modeling Approach	Environment	Scenario	Channel Characteristics	No. of Bounces	Operating Wavelength
[32]	1979	Cavity Model	Empty rectangular small office, large office and hall	Diffuse	$H(0)$, μ_τ	1	NIR IRED (λ= 950 nm)
[75]	1993	Recursive Method	Empty conference room	NDLoS and diffuse	$h(t)$, $H(f)$	3	NIR LD (λ= 832 nm)
[113]	2002	Recursive Method	Empty rectangular room	NDLoS	$H(0)$, SNR	0	White LED (λ= 380−780 nm)
[115]	2004	Recursive Method	Empty rectangular room	NDLoS and diffuse	$H(0)$, SNR	2	White LED (λ= 380−780 nm)
[95]	2002	Iterative Method	Rectangular room with arbitrary number of boxes	Diffuse	$h(t)$, PL	10	NIR LD (λ= 832 nm)
[87]	1997	DUSTIN	Empty rectangular room	Diffuse	$h(t)$	$1 \geq$	NIR LD (λ= 832 nm)
[67]	1997	Ceiling-Bounce Model (CBM)	5 Offices and single large room	NDLoS and diffuse	$h(t)$, $H(f)$, D_{rms} PL, Shadowing	1	NIR LD (λ= 832 nm) and (λ= 806 nm)
[105], [112]	2008, 2009	Modified Ceiling-Bounce Model (MCBM)	2 Empty rooms of different sizes	Diffuse	$h(t)$, $H(0)$, $H(f)$ D_{rms}, μ_τ, PL	1	NIR IRED (λ= 800−900 nm)
[118]	2015	Ceiling-Bounce Model (CBM)	Furnished rectangular rooms	NDLoS	$h(t)$	1	White LED (λ= 380−780 nm)
[106]– [108]	2014– 2016	Ray-tracing (Zemax®)	Empty/furnished rooms of different sizes and shapes	NDLoS	$H(0)$, D_{rms}, μ_τ	$1 \geq$	White LED (λ= 380−780 nm), NIR IRED (λ= 880 nm)
[102]	2013	Ray tracing	Sports utility vehicle	NDLoS and diffuse	$h(t)$, $H(f)$, D_{rms}	N/A	NIR IRED (λ= 1330 nm)
[100]	1998	Monte Carlo Algorithm	2 Empty rooms of different sizes	Diffuse	$h(t)$, D_{rms}	40	NIR LD (λ= 832 nm)
[101]	1998	Modified Monte-Carlo Algorithm	2 Empty rooms of different sizes	Diffuse	$h(t)$, D_{rms}	40	NIR LD (λ= 832 nm)
[78]	2009	Modified Monte-Carlo Algorithm (Rhinoceros® 3D)	Aircraft cabin	NDLoS and diffuse	PL	N/A	NIR IRED (λ= 870 nm)
[138]	2010	Modified Monte-Carlo	Empty rectangular room and cubic furnished office	NDLoS	$h(t)$, $H(f)$, D_{rms}	4	White LED (λ= 380−780 nm)
[61] [103]	2002	Spherical Model	Rectangular empty lab	Tracked and diffuse	$H(f)$, PL	$1 \geq$	NIR LD (λ= 993 nm)
[124] [123]	2012, 2014	Spherical Model	Empty office room	NDLoS and diffuse	$h(t)$, $H(f)$	$1 \geq$	White LED (λ= 380−780 nm)
[125]	2005	Carruthers Model	11 Empty rooms of different sizes	NDLoS and diffuse	$H(0)$, D_{rms}, μ_τ	3	NIR IRED (λ= 800−900 nm)
[86]	2007	HAYASAKA-ITO Model	Empty rectangular room	Diffuse	$h(t)$, $H(f)$, PL	1st, $3 \geq$	NIR LD (λ= 784 nm)
[131]	2016	RS-GBSM (One-Ring)	Furnished Office room	NDLoS	$h(t)$, $H(0)$, D_{rms}, μ_τ, K_{rf}	1	White LED (λ= 380−780 nm)
[111]	2016	RS-GBSM (two-ring and ellipse)	Furnished Office room	NDLoS	$h(t)$, $H(0)$, D_{rms}, μ_τ, K_{rf}	3	White LED (λ= 380−780 nm)
[109] [77]	2015 2017	Ray-tracing (Zemax®)	Empty/furnished rooms of different sizes	NDLoS	$h(t)$, $H(0)$, D_{rms} μ_τ, B_c, PL	8: Diffuse 14: Specular	White LED (λ= 380−780 nm)

SNR: signal-to-noise ratio; RS-GBCM: regular-shaped geometry-based channel model; N/A: not applicable

OTx can be modeled using a generalized Lambertian radiation pattern as [32]

$$R(\phi) = \frac{m+1}{2\pi}\cos^m(\phi), \phi \in [-\pi/2, \pi/2]. \qquad (10)$$

Here, ϕ is the angle of irradiance which is commonly denoted as the angle of departure (AoD) and m is mode number of the radiation lobe, which specifies the directionality of the optical source. At the receiving side, the ORx is modeled as an active area A_{R} collecting radiation which is incident at angle θ smaller than the PD's FoV. The incident angle is commonly denoted as the angle of arrival (AoA). Therefore, the received optical signal is proportional to $A_{\mathrm{R}} \cos(\theta)$. Only rays that are incident within ORx FoV

will be captured. For a particular optical source **S** and optical receiver **R** in a room with Lambertian reflectors, light from the OTx can reach the ORx through direct or multiple paths (number of bounces). Therefore, the CIR $h(t)$, scaled by time domain, can be expressed as the superposition of the LoS and an infinite sum of multiple-bounce components as [10]

$$h(t; S, R) = h^0(t; S, R) + \sum_{k=1}^{\infty} h^k(t; S, R). \qquad (11)$$

Here, $h^k(t)$ is the CIR of the components undergoing exactly k reflections. The LoS response h^0(t) is approximately a
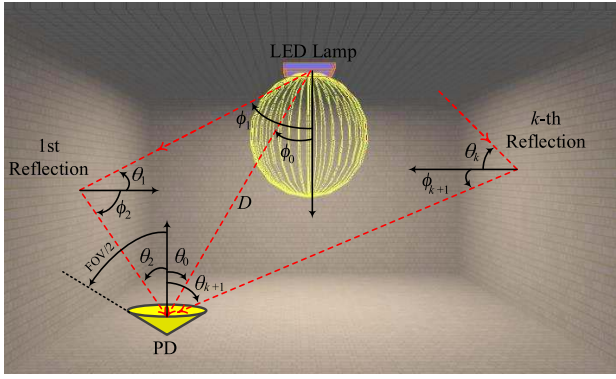
Fig. 4.   Recursive model.

Fig. 5.   Recursive and Iterative models.

scaled and delayed Dirac delta function expressed as [75]

$$h^0(t) \approx \frac{(m+1)A_R}{2\pi D^2} \cos^m(\phi)\cos(\theta)\delta(t - D/c). \quad (12)$$

Here, D and c are the OTx-ORx distance and the speed of light, respectively. The recursive approach is used to solve a given problem by breaking it up into smaller pieces, solve it and then combine the results. Therefore, the implementation of this algorithm is done by breaking the reflecting surfaces into numerous small Lambertian reflecting elements ε (cells), each with an area ΔA as shown in Fig. 4. Each cell plays the role of both an elemental receiver (ε^r) and an elemental source (ε^s). Accordingly, $h^k(t)$ for higher-order terms ($k > 0$) can be calculated recursively and approximated as [75]

$$\begin{aligned}
h^k(t; S, R) &\approx \sum_{i=1}^{N} \rho_{\varepsilon_i^r} h^{(0)}(t; S, \varepsilon_i^r) \circledast h^{(k-1)}(t; \varepsilon_i^s, R) \\
&= \frac{m+1}{2\pi} \sum_{i=1}^{N} \frac{\cos^m(\phi)\cos(\theta)}{D^2} \\
&\quad \times \text{rect}(2\theta/\pi) \, h^{(k-1)}(t - D/c; s_i, R)\Delta A.
\end{aligned}$$
$$(13)$$

Here, N, ρ and s_i denote the number of cells, cell reflectivity coefficient, and the position of each cell, respectively. According to (13), in order to calculate $h^k(t; S, R)$, firstly, all possible $h^{(k-1)}(t; \varepsilon_i^s, R)$ must be calculated. Then directly apply (13) for the intended OTx. Fig. 5(a), illustrates Barry's approach for computing the CIR $h^{(k)}$ of multiple bounce ($k > 0$) recursively. For example, if ($k = 3$), $h^2(t; S, R)$ can be obtained by first computing N impulse responses of $h^1(t; \varepsilon_i^s, \varepsilon_i^r)$. Using these to compute $h^2(t; \varepsilon_i^s, R)$. The latter result then directly applied to (13) for the intended OTx.

After a gap of ten years, Barry's model in WIRCs has been extended to model NDLoS VLC channels, e.g., [113]–[115]. Barry's model has been first extended for VLC channels in order to make use of the existing power-line network for VLCs [113]. The same researchers of the latter work have adopted Barry's model in VLCs considering up to second order reflections [115]. The previous study discussed the effect of SNR and ORx FoV on data rate. Thereafter, many studies utilized the recursive model for VLC systems, such as [47] and [73]. An improved recursive channel model for
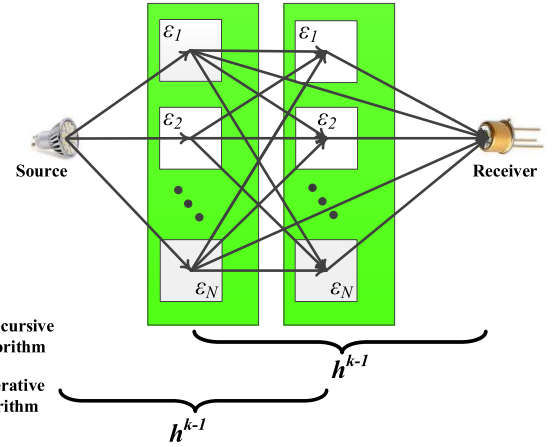
VLCs is presented in [116]. This model considers the total path length including electrical signal path passing through a wiring topology in addition to the optical wireless path. Lee *et al.* [114] generalized the Barry's model by including wavelength-dependent WLED characteristics and spectral reflectance of indoor reflectors. Their study showed that VLCs provide larger transmission bandwidth compared with WIRCs. It is worth mentioning that recursive model is still used for VLCs channel modeling so far, e.g., [97]. In recursive approach, although the reliability of results improves with the number of reflections taken into account, the computing time increases exponentially [61]. On the other hand, when too few reflections are taken into account, PL and bandwidth are systematically overestimated.

b) Iterative model: Iterative based algorithm was introduced in [95] by Carruthers and Kannan. In this method, CIR $h(t)$ calculation follows the basic methodology that outlined in [75] with extensions for an arbitrary number of boxes inside the environment. The LoS CIR $h^0(t)$ can be computed using (12). While, the k-bounce response $h^k(t)$ is given as

$$h^k(t; S, R) \approx \sum_{i=1}^{N} \rho_{\varepsilon_i^r} h^{(k-1)}(t; S, \varepsilon_i^r) \circledast h^0(t; \varepsilon_i^s, R). \quad (14)$$

According to iterative algorithm, (14) can be applied with $R = \varepsilon_j^r$ to get

$$h^k(t, S, \varepsilon_i^r) = \sum_{j=1}^{N} \alpha_{ij} h^{(k-1)}\left(t - D_{ij}/c; S, \varepsilon_j^r\right) \quad (15)$$

where

$$\alpha_{ij} = \text{rect}(2\theta/\pi) \, \frac{\rho_{\varepsilon_j^r} \cos^m(\phi_{ij})\cos(\theta_{ij})}{P^2 D_{ij}^2}. \quad (16)$$

Here, the quantities ϕ_{ij}, θ_{ij}, D_{ij}, and P denote the source's angle to the receiver, the receiver's angle to the source, the source (ε_i^s)-receiver (ε_j^r) distance, and cells spatial partitioning factor, respectively. For example, if ($k = 3$), $h^2(t; S, R)$, can be obtained by first computing N impulse responses of $h^1(t; S, \varepsilon_i^r)$. Using these to compute $h^2(t; \varepsilon_i^s, \varepsilon_j^r)$. The latter result then directly applied to (14) for the intended ORx.

Fig. 5(b) illustrates iterative algorithm. It has been reported that the iterative method is about 92 times faster compared with recursive method when three-bounce considered [95].

c) DUSTIN algorithm: In order to reduce the computational complexity of the previous models, López-Hernández and Betancor [87] developed an efficient simulation approach called DUSTIN algorithm. Similar to recursive and iterative models, this approach was based on a discretization of the reflecting surfaces into cells. However, in DUSTIN approach, the simulation has been done by slicing into time steps rather than into a number of reflections. This method was proposed to simulate the CIR $h(t)$ of indoor WIRCs. DUSTIN algorithm was considered faster compared with traditional iterative and recursive approaches [117]. For instance, in the recursive approach, the time required to compute $h^k(t)$ is roughly proportional to N^k [75], while it is proportional, in the DUSTIN algorithm, to N^2 and hence get the advantage of simulating any number of reflections. However, the drawback of this approach is that it is incapable of adapting to different environments. This is due to wireless channel part calculations are saved in a disk file before calculating the response of the ORx and hence it is considered as a site-specific model. DUSTIN approach, on the other hand, has not been utilized in VLCs so far.

d) Ceiling bounce model (CBM): This model came up with a closed-form solution for the CIR $h(t)$, PL, and D_{rms} of diffuse indoor WIRC channels [10], [67]. It was assumed that the OTx and ORx are collocated. It is the most used approach in simulation because of its excellent matching with the measured data and simplicity. Based on this model, WIRC channels can be characterized only by the optical wireless channel PL and D_{rms}. The diffuse CIR $h(t)$ based on CBM is given as [67]

$$h(t, a) = H(0) \frac{6a^6}{(t+a)^7} u(t). \tag{17}$$

Here, $u(t)$ is the unit step function and a is environment related parameter, $a = 2H_c/c$, where H_c is the height of the ceiling above the OTx and ORx. The delay spread and approximate 3-dB cut-off frequency for the CBM are given by the following relations $D_{\text{rms}} = \frac{a}{12} \sqrt{\frac{13}{11}}$ and $f_{3-\text{dB}} = \frac{0.925}{4\pi D_{\text{rms}}}$, respectively. It has been noticed that this model can be more realistic with multiple reflections and it accurately models the relationship between D_{rms} and multipath power requirement for diffuse shadowed and unshadowed channels by modifying a as detailed in [67]. On the other hand, when the LoS path dominates, the unshadowed LoS CIR $h(t)$ can be computed, based on cavity model, as [32]

$$h(t) = \frac{A_R H^2}{\pi D^4} \delta(t - D/c). \tag{18}$$

Here, H is the vertical OTx-ORx separation. The OTx is a Lambertian of first-order and it is pointed down, while the ORx is pointed up. For being simple and easy to use, CBM has been employed in VLCs. For example, Wang and Chen [118] utilized CBM to propose a grouped discrete Fourier transform (DFT) precoding scheme for reduction of peak-to-average power ratio (PAPR) for orthogonal frequency division multiplexing (OFDM)-based VLC systems.

e) Geometry-based deterministic models (GBDMs) based on ray-tracing: Most advanced ray-tracing tools are based on the theory of geometrical optics (GO) and the uniform theory of diffraction (UTD) [119]. Ray-tracing computing all rays for each receiving point individually, which is the most time-consuming part of a prediction based on this method. For instance, in WIRCs, PL estimation requires about 10^8 trials while estimating the CIR $h(t)$ takes up to 10^{10} trials with subnanosecond time resolution [103]. Based on a specific ray-tracing software, ray-tracing guarantees the specifications of the created environment including geometry, furnishing, and the reflection characteristics of the surface materials as well as the specifications of the OTx and ORx. There is a wide range of available free and licensed ray-tracing software and their platform operating systems (OS) are listed in [120]. Moreover, as will be seen later in this subsection, some site-specific ray-tracing software that developed in the field of image processing or illumination design purposes may be useful for optical wireless channel modeling. In [104], ray-tracing based channel modeling showed similar results as Barry's recursive model when the simulation is stopped after three reflections. Furthermore, ray-tracing based on ray-quadrilateral intersection algorithm was proposed for intra-vehicle channel modeling in order to investigate WIRC channel's characteristics in a sport utility vehicle (SUV) of 15-passenger capacity [102].

On the other hand, a pure ray-tracing based channel modeling for VLCs has recently presented in [106]. In order to express the CIR $h(t)$ of NDLoS indoor VLC links in rectangular empty rooms of different sizes, the authors exploited the ray-tracing features of a licensed optical software called Zemax$^{\text{Zemax}}$. Originally, Zemax is windows-based software able to create a three-dimensional (3D) indoor environment where the main purpose of such software is optical and illumination system design. The data which are created by Zemax are imported into MATLAB to produce the CIR $h(t)$ through considering a proper normalization. The same work has been extended to consider empty rooms with L-shaped and circular shape, furnished rooms, and different wall materials, i.e., brick, wood, and plaster [107]. This approach has been validated against the recursive model in [114] as shown in Fig. 6. It can be observed that the CIRs are almost identical when considering first three reflections, i.e., $k = 3$. The small differences between the tails are due to the fact that light source which is used in [107] and [109] is a commercial light source and not ideal Lambertian, unlike the theoretical light source in [114]. More generalized study for indoor VLC channel modeling is conducted in [108] including 15 different NDLoS links. The latter studies have demonstrated that the presence of furniture leads to decrease channel DC gain $H(0)$ and D_{rms}. Furthermore, based on comparisons between WIRC and VLC channels, the results further reveal that, for the same configurations, DC gain and D_{rms} of WIRC channels are larger than that of VLC channels. In [109], ray-tracing using Zemax
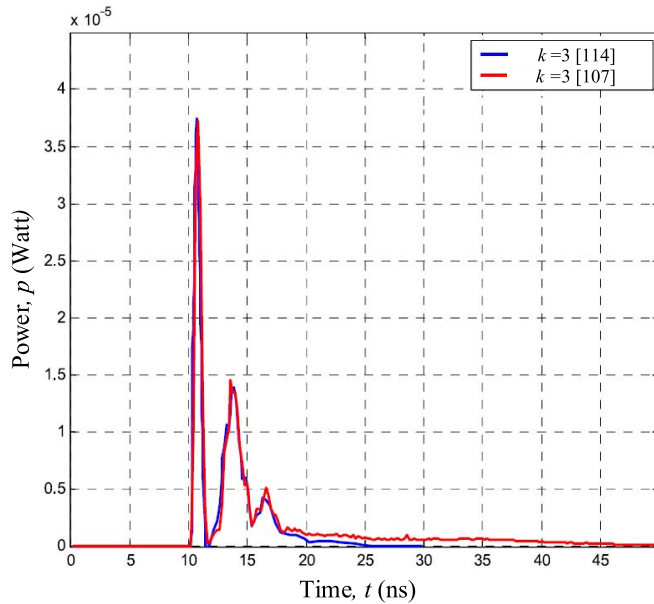
Fig. 6.   Comparison of GBDM based on ray-tracing in [107] with recursive model in [114].

has been used for VLC channel modeling considering $k = 8$ in the case of purely diffuse reflections and $k = 14$ in the case of mostly specular reflections. In that study, the relation between coherence bandwidth B_c and D_{rms} (for IR and visible light channels) was expressed through curve-fitting. While Miramirkhani *et al.* [77] have extended the work in [109] to model the PL of visible light channels. Based on the above facts, ray-tracing requires a detailed description of the propagation environment and consequently cannot be easily generalized to a wider class of scenarios, therefore, it is also considered as a site-specific model.

2) Stochastic Channel Models: In stochastic models, the impulse responses of OWC channels are characterized by the law of wave propagation applied to specific OTx, ORx, and scatterer geometries, which are predefined in a stochastic fashion according to certain probability distributions. Compared to the deterministic, the stochastic approach offers increased flexibility, reduced computational complexity, and considered as non site-specific but with lower accuracy.

a) GBSM:

1) *The Spherical Model:* This model was proposed to model WIRCs channels that utilizing diffused link configurations. The model provides a quick rule of thumb in order to approximate prediction of optical wireless channel PL and $H(f)$ for the higher order reflections in indoor environments [61], [103], [104]. This model is inspired by the traditional approach of integrating sphere (IS) photometry which is introduced in [122]. A simple analytic formula for CIR $h(t)$ is derived from the integrating sphere and scaled to a specific room as detailed in [103]. Still, the LoS CIR $h^0(t)$ can be computed using (12). While, according to spherical model, the diffused CIR $h_{diff}(t)$ is given as [10]

$$h_{diff}(t) = \frac{H_{diff}}{\tau} \exp(-t/\tau). \qquad (19)$$

Apparently, the CIR $h_{diff}(t)$ is exponential with decay time τ. The term H_{diff} denotes diffused channel gain, which is expressed as

$$H_{diff} = \frac{A_R}{A_{room}} \frac{\rho}{\langle \rho \rangle}. \qquad (20)$$

Here, the paramerers A_{room} and $\langle \rho \rangle$ denote the room area and the average reflectivity, respectively. The latter parameter is defined as [61]

$$\langle \rho \rangle = \frac{1}{A_{room}} \sum_i \Delta A_i \times \rho_i. \qquad (21)$$

Here, the individual reflectivity ρ_i of the cells weighted by their individual areas ΔA_i. Furthermore, the corresponding channel PL and $H(f)$ have been derived. By using spherical model, it is shown that a highly reflective geometry resulting in a high delay spread, hence low channel bandwidth. In contrast, if the geometry reflectivity is low, this leads to low delay spread and thus high channel bandwidth. The reliability of the spherical model for WIRC channels for the higher order reflections has been confirmed by stochastic based ray-tracing simulation, which takes all diffuse reflections into account [61], [103]. The spherical model, on the other hand, has been employed to investigate VLC channel characteristics based on a new design of LED lighting [123]. While in [124], the accuracy of the spherical model for VLC channels has been examined compared with Barry's model. The simulation results showed that the impulse response of the diffuse portion was overestimated when considering the spherical model. Furthermore, the diffuse portion has no much influence on 3-dB bandwidth.

2) Carruthers Model: In this model, the channel responses were generated based on geometrical modeling of indoor environments together with an iterative technique for calculating multiple reflections [125]. A comprehensive study has examined the characteristics of more than 80000 CIRs of indoor WIRC channels, which are generated using a channel simulator called infrared impulse response simulator by iteration (IrSimIt) [126]. It has been demonstrated that LoS channels must be modeled separately from those fully diffuse channels, which have no such path. Compared to [91], the study declared that the LoS channel gain following a modified gamma distribution (MGD) for D < 0.4 m. While the channel gain for LoS channels including all reflections, follows a modified Rayleigh distribution (MRD) for most OTx-ORx distances. The channel gain is measured in decibel (dB) and the fitting process is carried out using chi-square (χ^2) goodness test. Furthermore, the study has recommended a roadmap for generating a stochastic realistic impulse response for any given OTx-ORx separation in an indoor environment. On the other hand, Carroll [127] have followed the similar methodology to that used in [125] to model the channel gain and D_{rms} of diffuse channels. They showed that the shifted lognormal distribution was the best distributions to model diffuse channel gains while the gamma distribution was the best for diffuse D_{rms}.

3) RS-GBSMs: These models are widely used in RF channel modeling, e.g., [128]–[130]. In this model, the effective

scatterers are located on regular shapes, such as a ring, an ellipse [69] or even a combination of both as reported in [128], in case of two-dimensional (2D) models. While in case of 3D models, the effective scatterers are lying on a sphere or an ellipsoid, e.g., [129] and [130]. Different from physical scatterers, an effective scatterer may include several physical scatterers which are unresolvable in delay and angle domains [130]. RS-GBSM is a mathematically tractable approach, therefore, it has been employed in VLCs. Al-Kinani *et al.* [131] used the one-ring model to investigate indoor VLC channel characteristics. The results have been verified with [75] (configuration A). In [111], a combined two-ring and an ellipse model was proposed to model indoor VLC channels. The simulation has shown comparable results with [58] up to three reflections.

b) Non-GBSMs:

1) *Monte Carlo Algorithm (MCA):* After a year of introducing DUSTIN algorithm, the same working group has introduced MCA in order to further reduce the intensive computational effort required to compute the CIR $h(t)$ for indoor WIRC channels [100]. In MCA, the generalized Lambertian radiation pattern is assumed and the same link configurations in [75] and [87] (configuration A), are employed in order to compare the results. The simulation in this method is neither sliced into a number of reflections as in [75], nor in time steps as in [87]. It can be implemented through three steps: ray generation, wall processing, and calculation of the PD response. MCA allows evaluation of impulse response for not only Lambertian ($m \geq 1$) but also specular reflections. The computational complexity and simulation time of Monte Carlo approach is less compared with the recursive and DUSTN models [117]. However, the main drawback of MCA is that, for a regular sized room, it requires to send many more rays than the number that will be received. This is because that not all rays will be intercepted by the ORx. Therefore, the same working group has developed MCA approach as detailed in the next subsection.

2) *Modified Monte Carlo algorithm (MMCA):* López-Hernández *et al.* [100] developed MCA and came up with a mixed ray-tracing-Monte Carlo algorithm for simulating multipath response for indoor WIRC channels [101]. The new method called modified Monte Carlo algorithm (MMCA) which is faster and more accurate than classic Monte Carlo method. This is due that MMCA ensures that each ray contributes to the final channel response function each time it bounces off an obstacle. MMCA was more accurate and faster enough to calculate the room dispersion within few minutes, which is 20 times faster than DUSTIN algorithm [68]. In contrast with the recursive model [75], MMCA, is faster and more concise algorithm to simulate the CIR $h(t)$ for indoor WIRC channels. Its computational complexity is kNN_r, where N_r is the number of rays [132]. MMCA is preferable in terms of reliability but might be less efficient than cavity model [61]. In [133], MMCA is extended to examine Phong reflection model that presented in [134]. Simulation results showed that the use of Phong model can lead to differences compared to Lambert model in the evaluation of the impulse response when surfaces exhibit a high specular component. Furthermore, the discretization error due to the number of random rays produces an error in computing the impulse response in MMCA. It has been verified that the error is proportional to $1/\sqrt{N_r}$ [135]. An algorithm for estimating the error in computing the impulse response has been reported in [136]. The latter algorithm can account for any number of reflected paths, irregularly shaped rooms, furniture, specular and diffuse reflectors. The use of bidirectional reflectance distribution function (BRDF) on MMCA is reported in [137]. This is allowed for more general and accurate modeling of the reflection properties of the different reflecting surfaces. In terms of channel modeling of WIRCs in transportation means, Dimitrov *et al.* [83] adopted Monte Carlo ray-tracing simulation in order to estimate the PL of WIRC channels inside an aircraft cabin. The simulation is performed based on a geometric computer-aided design (CAD) cabin model. On the other hand, in terms of VLCs, MMCA based on the Lambert-Phong pattern for single source and multiple source systems is presented in [138]. The simulation results showed that when using the Lambert-Phong reflection pattern, the calculation becomes linear to the number of reflections and the computation complexity is decreased.

3) *Modified Ceiling Bounce Model (MCBM):* The traditional CBM, however, ignored (as an approximation) the contribution of the walls to the total CIR $h(t)$. Therefore, Smitha *et al.* [105] developed a modified CBM (MCBM) based on combining the traditional CBM in [67] with the stochastic model in [91]. MCBM presents a more accurate CIR $h(t)$ with less computational complexity compared to the traditional CBM [112].

4) *HAYASAKA-ITO Model:* According to this model, the CIR $h(t)$ of WIRC channels is decomposed into primary reflection $h^1(t)$ ($k = 1$) impulse response and higher-order reflections $h^{\text{high}}(t)$ ($k \geqslant 3$) impulse response [86]. Based on the used link design, the second-order reflection has been neglected. The authors have selected Gamma distribution to model $h^1(t)$ and hence the normalized impulse response is given as [10]

$$h^1(t) = \frac{\beta^{-\alpha}}{\Gamma(\alpha)} \, t^{\alpha-1} \, \exp\left(-\frac{t}{\beta}\right). \tag{22}$$

Here, $\Gamma(\alpha)$ is the Gamma function while α and β are characteristic parameters related to the physical parameters of the channel. On the other hand, $h^{\text{high}}(t)$ has been modeled using spherical model that was mentioned previously. The most important outcomes of HAYASAKA-ITO model, that it has demonstrated that the bandwidth characteristics are dominated by the response of the primary reflection rather than the higher-order reflections, and the PL within the communications range does not depends on the FoV of the ORx.

VI. Outdoor OWCs Channel Models and Measurements

There is a wide diversity in the field of outdoor OWCs applications including IR free space communications and VLCs. IR free space communication is mature technology and IR free space channels have been comprehensively studied [10]. However, outdoor VLC applications have become a hot topic

recently, especially in vehicular ad hoc networks. Vehicular networks enable the cars to exchange information that may be useful in facilitating road safety in order to create an accident-free environment. Over the last few years, we have witnessed many research efforts towards the adaptation of R2V, V2R, and V2V communications to the intelligent transportation systems (ITS). Furthermore, nowadays, the research efforts have been directed towards what so-called vehicle to everything (V2X) technology. This includes V2V, R2V, V2R, vehicle-to-device (V2D), vehicle-to-pedestrian (V2P), vehicle-to-home (V2H), and vehicle-to-grid (V2G) communications [139].

Recently, vehicular ad-hoc network (VANET) technology provides tremendous potential to improve road safety, traffic efficiency, and ensure the safety and convenience of drivers, passengers, and pedestrians [140]. VANET utilizes dedicated short-range communication/wireless access in vehicular environment (DSRC/WAVE) standard for fast data communication [71]. In order to implement DSRC/WAVE, new hardware need to be added. However, adding more hardware to the infrastructures and cars is always an issue in terms of cost and power consumption. Therefore, the idea is to take advantage of VLC technology in vehicular communications to introduce what so-called vehicular VLCs (VVLCs). In order to adopt VLCs in the ITS, detailed knowledge about the underlying propagation channel is indispensable to get optimum link design and performance evaluation.

GBDMs have been widely used in VVLCs in terms of R2V scenarios, such as traffic light control at intersections [141]–[145] considering only the LoS channel between the OTx and the ORx. A deterministic VVLC V2V and V2R channel models based on the ray-tracing method was proposed in [110] and [146]. This model requires a detailed and time-consuming description of the propagation environment and consequently cannot be easily generalized to a wider class of scenarios. Luo *et al.* [147] used geometry-based road-surface reflection model, which considers LoS and NLoS components. The latter model ignored all other reflections except that reflected off the road-surface, i.e., asphalt. Furthermore, the model utilized a market weighted headlamp (i.e., tungsten halogen headlamp) beam pattern model rather than LED-based Lambertian radiation pattern. The same authors have extended the previous model to establish a 2×2 VVLC MIMO system [148]. Most recently, Al-Kinani *et al.* [149] have proposed a RS-GBSM for VVLC channels, which has the ability to consider the LoS and NLoS components. The proposed model has already considered the light that reflected off moving vehicles around the OTx and ORx and the stationary roadside environments.

On the other hand, in terms of VVLC channel measurements, it has been noticed that there is a considerable amount of channel measurements campaigns available in the literature. The feasibility of realizing VVLC networks in daytime conditions has been examined in [150] under constraints posed by noise, interference, and multipath. Commercial WLEDs and PDs have been utilized, and in order to increase the robustness against ambient noise, the PD has been amounted inside a case with a front aperture where a 4x zoom optical lens has been placed. Based on testbed measurements and simulations, the reachability and latency for V2V, R2V,

and V2R communications scenarios have been investigated. Lourenco *et al.* [151] have developed VVLC prototype based on direct sequence spread spectrum/sequence inverse keying (DSSS/SIK) modulation technique to minimize the effect of external noise sources. By using commercial WLEDs and PIN PD, the simulation experimental results have demonstrated that it is feasible to achieve more than 40 m LoS communication range for low data rate applications even in the presence of significant optical noise levels. In [63], the authors proposed using a maximal ratio combining (MRC)-based receiver diversity technology in VVLC to improve the system performance and increase transmission distance. The measurements carried out using a testbed composed of commercial RGB LED or WLED and two commercial APDs on a clear summer night (no sunlight noise) to demonstrate the feasibility of the proposed VVLC LoS link over 100 m. Most recently, four LEDs traffic lights R2V testbed has been presented in [152] utilizing red LEDs and Si wideband amplified detector operating in the daytime condition. System performance has been investigated over three trajectories, i.e., forward, right turn, and left turn. The proposed system based on spread spectrum/pulse-position modulation (PPM) modulation technique. The experimental results showed that the proposed system can achieve seamless switching between four-way LED traffic lights at the intersection over up to 15 m.

According to the literature, there are still many remaining challenges that are not yet addressed in VVLC systems. Such challenges include weather conditions impact, temperature, and multipath interference. Therefore, further theoretical and experimental work are necessary.

VII. Underwater OWCs (UOWCs) Channel Models and Measurements

Underwater communications (UWCs) refer to transmitting data in water environment by the means of wireless carriers, i.e., RF, acoustic waves, and optical waves. UWCs based RF require huge antenna size, costly, and energy-consuming transceivers in fresh water and suffers from high attenuation in seawater due to the conductivity of seawater. Thus, the best alternatives to UWCs based RF systems are wireless acoustic and optical techniques. Acoustic techniques represent a relatively mature and robust technology. The key advantage of underwater acoustic communications (UACs) that they used to realize a long-distance communication link range up to several tens of kilometers [23]. However, acoustic communications have limited bandwidth (typically on the order of Kbps), limited data rates, and significant latency due to the slow propagation speed of the sound wave in the water (about 1500 m/s for pure water at 20 Celsius) [153]. In recent years, there is growing research activities in UWCs and underwater sensor networks (UWSN) that require high-speed and reliable links for underwater missions such as employing robotics, AUV, and remotely-operated vehicles (ROV). This triggers the demand for UOWC links exploiting the fact that the ocean is relatively transparent in the visible light spectrum and attenuation property takes its minimum value in the blue-green spectral range (450 – 550 nm). Compared to UACs, UOWCs offer higher transmission data rates (on the

order of Mbps to Gbps), low latency, higher energy efficiency, lowest implementation costs, and also has much less impact on marine animal life [23], [71], [154]. Therefore, UOWC have been suggested as a viable alternative or complementary to the existing UAC systems. However, UOWC realize shorter communication links on the order of 100 – 200 m, and up to 300 m in the clearest water [155]. As a matter of fact, since they utilize the visible band, UOWCs have been referred to in the recent literature as underwater visible light communications (UVLCs).

The characteristics of aquatic channels are determined by the optical properties of water, objects, and suspended particles. Examples of such water properties are pressure, the flow, temperature, and salinity, in addition to the size of objects. Consequently, underwater channels considered as the most complex and harsh channels in nature [156]. For simplicity, several researchers utilized the Beer-Lambert's law to model the LoS UOWC channels [157]–[159]. According to Beer-Lambert's law, the attenuation loss (i.e., PL) is calculated by [154]

$$\text{PL}_{\text{BL}} \text{ (optical dB)} = 10 \log_{10} \exp(-\kappa(\lambda)D). \quad (23)$$

Here, D is the OTx-ORx distance and $\kappa(\lambda)$ stands for the attenuation coefficient. However, Beer-Lambert model has been reported as inaccurate since it contains implicit assumptions make it overestimates the PL [160]. Alternatively, underwater light propagation is modeled by the radiative transfer equation (RTE) which expresses the energy conservation of a light wave traversing a scattering medium. The vector RTE is given as [24]

$$\left[\frac{1}{c} \frac{\partial}{\partial t} + \mathbf{n} \cdot \nabla \right] I(t, \mathbf{r}, \mathbf{n}) = \int_{4\pi} \xi(\mathbf{r}, \mathbf{n}, \mathbf{n}') \ I(\mathbf{r}, \mathbf{n}, \mathbf{n}') \mathrm{dn}' \\ - \kappa(\lambda) \ I(t, \mathbf{r}, \mathbf{n}) + E(t, \mathbf{r}, \mathbf{n}). \quad (24)$$

Here, $\mathbf{n}$ is the direction vector, $\mathbf{r}$ is the position vector, ∇ is the divergence operator with respect to $\mathbf{r}$, I is the irradiance in W/m^2, E is an internal source radiance (e.g., sunlight) in W/m^2 sr, ξ is the volume scattering function (VSF), which is defined in [24].

The derivation of RTE is complex and it can be solved both analytically and numerically. Several attempts to solve RTE analytically have been reported such as [161] and [162]. In order to find the analytical solutions, a series of assumptions and approximations need to be introduced to simplify RTE. Therefore, the analytical solutions suffer from numerous limitations [163]. Instead, most researchers have focused on developing a powerful numerical method to solve RTE. The most popular numerical approach to solve RTE is Monte Carlo simulation [23].

Monte Carlo based channel modeling has been widely used to characterize UOWC channels [153], [164]–[167]. In [164], based on Monte Carlo simulations results, a statistical inference process has been made to find the best-fitting option for the CIR $h(t)$ and D_{rms}. Gabriel *et al.* [153] considered five different water types of empty underwater environment. The study investigated the effect of the ORx's lens aperture

size, the impact of link distance, and the impact of the OTx parameters.

Since turbulence is typically non-negligible in a practical seawater environment, Dong and Liu [168] combined stochastic model and log-normal turbulence model. Then the performance of the proposed UOWC multiple-input single-output (MISO) system has been evaluated in the presence of weak turbulence as well as absorption and scattering. Zhang *et al.* [169] presented a stochastic model for UWOC links by adopting the Henyey-Greenstein (HG) function as probability density function (PDF) of scattering angle. The study considered non-scattering and single scattering components of UWOC links. The study in [169] has been further extended by the same research group to take into account multiple scattering components when considering long communication distance and/or more turbid water type [170]. The most recent work on UOWC channel modeling is presented in [154], taking into account the presence of divers and AUV to investigate the effects of shadowing and blockage. The authors utilized ray-tracing Zemax tool to characterize UOWC channels. Table V presents the most indicated UOWC channel models in the same style of aforementioned tables, but further considering water type.

In terms of UOWC channel measurements, an early experimental work has been conducted in freshwater and coastal seawater in 1992 [171]. The authors utilized three types of lasers and two types of receivers to investigate spatial and temporal propagation characteristics of the LoS UOWC channels. The used lasers are continuous-wave (CW) argon-ion laser (514 nm) and two CW and pulsed Nd:YAG lasers (532 nm). While the receivers were APD and PMT. The first utilization of LEDs for LoS UOWC is proposed in [172]. Two blue and red LEDs (450 nm and 660 nm, respectively) have been used in clear ocean water and turbid water. The experimental work demonstrated that a 10 Mbps can be achieved over ranges up to 20 m in dark clear ocean water considering APD at the receiver. In order to verify the Monte Carlo approach for UOWC channel modeling, an experimental testbed that consists of a 2 m water pipe has been reported in [173]. The testbed consists of a green LD (532 nm), beam splitter (BS), integrating sphere to measure the intensity of the light transmitted through the water pipe, in addition to APDs. Experimental results exhibited a reasonable agreement in terms of channel frequency response in three different types of waters, i.e., clear ocean, coastal ocean, and harbor water. Cox and Muth [174] presented a similar verification of Monte Carlo approach utilizing the same optical source and water types in [173] but in water tank rather than a pipe. The study investigated UOWC channel losses considering the distance, ORx aperture size, and FoV. Cochenour *et al.* [161] have derived a mathematical model for beam-spread function (BSF) which describes the propagation of a laser source through water in the presence of scattering. Then an experiment used to measure the beam spread in a laboratory water tank to validate the aforementioned model utilizing green LD (532 nm) in turbid water. Besides the stochastic Monte Carlo approach, there are also deterministic methods that can be used to solve the RTE numerically but only a few researchers utilized

TABLE V
IMPORTANT UOWCs CHANNEL MODELS

Ref.	Year	Modeling Approach	Water type	Scenario	Channel Characteristics	Operating Wavelength
[157]	2005	Beer Lambert	Pure sea, turbid, clear ocean and gulf	DLoS	PL	LD (λ= 532 nm)
[164], [165]	2013, 2014	Monte Carlo	Clear sea	NDLoS	$h(t)$, $H(0)$, $D_{\rm rms}$, $B_{\rm c}$	LED (λ=470 nm & 660 nm)
[153]	2013	Monte Carlo	Pure sea, clear ocean, coastal ocean, turbid harbor, and estuary	NDLoS	$h(t)$, $D_{\rm rms}$	Green LED (λ=532 nm)
[166]	2014	Monte Carlo	Clear sea, Coastal, harbor	DLoS	$h(t)$, PL	LED (λ=400−600 nm)
[167]	2015	Monte Carlo	Coastal and harbor	Diffuse	$h(t)$, $H(f)$, PL	LD (λ=400−600 nm)
[175]	2015	Iterative	Coastal and harbor	NA	PL	NA
[168]	2016	Stochastic model	Clear sea	DLoS	$h(t)$, PL	LD (λ= 532 nm)
[169], [170]	2016	Stochastic model	Coastal	NDLoS and diffuse	PL	LD (λ= 532 nm)
[154]	2017	Ray-tracing (Zemax®)	Coastal	NDLoS and diffuse	$H(0)$, $D_{\rm rms}$, PL, shadowing and blockage	Blue LED (λ=450−480 nm)

deterministic models as alternatives to Monte Carlo simulation. For instance, Li *et al.* [175] proposed a fast numerical solution for RTE in order to calculate the UOWC channel path loss. Simulation results showed that the proposed scheme consuming shorter simulation time while keeping a comparable accuracy compared with Monte Carlo approach.

It is worth mentioning that in this paper we only consider fully UOWC channels since buoyant channels are out of the scope of this paper.

VIII. UNDERGROUND MINING COMMUNICATIONS (UMCs) CHANNEL MODELS AND MEASUREMENTS

Underground mining industry considered as one of the economic sectors that provide a significant boost to the global economy. However, underground mines are one of the most hazardous environments since they are composed of a network of tunnels that prone to collapse. More hazards are encountered due to the presence of toxic gases and substances resulting from mining and production, associated with the presence of dust [25]. Such environment requires reliable communications, monitoring and tracking systems that ensure safety and maximize productivity. Therefore, preserving information flow is one of the key challenges facing the mining industry during mining operations. This information includes detecting hazardous gases, smoke, monitoring mining machinery, and most importantly, monitoring miners and locating them when disasters occur. The most common communication systems in underground mines are node mesh, leaky feeder, and through-the-earth (TTE) [176]. Thus, information can be exchanged through wired or wireless communication or a combination of both. Wired communications utilize twisted pair, coaxial, and fibre-optic. However, the structure of underground mines is very complex. Therefore, wired communication systems are very susceptible to be damaged. On the other hand, the conventional wireless communication systems that are used overground cannot be directly applied in underground mines due to the high attenuation of radio

waves in underground mine galleries [177]. These challenges have inspired the researchers to think beyond the use of the classical communication systems taking into account that poor lighting condition in underground mines affects mining safety. This triggered the idea of using VLC technology to get the double benefit of improving lighting conditions and providing data transmission simultaneously in underground mines. In the literature, some researchers have introduced infrared, Bluetooth, ultra-wideband (UWB), and ZigBee to UMCs [178], [179]. However, VLC seems in some aspects superior to the later technologies for short range communications, i.e., $1 - 10$ m [111]. Since the employing of VLC technology in underground mining is still in a very early stage, it has been noticed that there are only a few researchers have focused on VLC channels characterization in underground mines, such as [79] and [180]–[181].

In general, the structure of in underground mines consists primarily of two areas, namely, mining roadway and workface. Therefore, the optical channel will be significantly affected by the mine structure. In [176], the recursive approach has been extended to investigate VLC channel characteristics in mining roadway and workface considering miner-to-miner (M2M) and infrastructure-to-miner (I2M) communication scenarios. Based on [176], the same research group further extend the recursive approach to investigate the optical PL considering three different trajectories [79], [181]. A GBDM is proposed in [180] taking into account the LoS component and the reflections from the roof, floor, left and right hydraulic support columns in coal mine workface. The study also considered the presence and the effects of coal dust on optical signal degradation. As VLC in underground mines still in early stage of development, very few experiment has been made to characterize optical channels in underground mines. For instance, Zhai and Zhang [180] have conducted experimental work to demonstrate the ability of VLC to deliver lighting and information within underground mining environments.

On the basis of the above, it can be concluded that the characteristics of the underlying VLC channels in underground

mines have not been sufficiently investigated yet and hence, more research efforts need to be tailored towards this issue especially for underground mines with complex structures.

IX. FUTURE RESEARCH DIRECTIONS IN OWCS CHANNEL MEASUREMENTS AND MODELS

This section is devoted to discussing important future research directions that can be considered as guidelines for conducting future OWCs channel measurement campaigns and developing more realistic channel models.

A. New Communication Scenarios

1) Aviation Environments: The aviation industry is another important area where OWCs can be applied. For WIRC systems, the PL exponent and the standard deviation of shadowing have been determined inside an aircraft cabin for specific scenarios [83]. However, channel measurements and modeling in the visible light spectrum are still of prime importance. This is due to the fact that VLC is a good candidate to connect the passengers to the Internet of aircraft things (IoAT) in the modern era of the aviation [182].

2) Smart Toy Communications: Smart toy networks can be used at homes or entertainment theme parks [183]. They utilize low-cost and energy-efficient LEDs operating in IR and visible light spectrums to create interactive communications for toy-to-toy, toy-to-smartphone/computer, and toy-to-environment. Such technology requires careful channel management in order to keep communication towards the desirable end devices.

3) Optical Body Area Network (OBAN): Transdermal optical communications have become a hot research topic recently due to the rapidly growing usage of implantable medical devices (IMDs) [71], [184]. In order to establish a communication link through a human body, the optical signal need to penetrate the skin layers. However, human skin is a complex biological structure, therefore, characterization of skin optical properties is an extremely challenging task.

B. MIMO VLC Channel Measurements and Models

MIMO VLC is a promising technology for future OWCs networks. This technology has been attracting researchers' attention due to its promising capability of greatly improving link reliability and high spectral efficiency (more bits/s/Hz) compared to IR LAN [10]. A 2×2 MIMO VLC configuration was demonstrated in [185], while a 4×4 configuration was presented in [186]. In this context, it is worth pointing out that for indoor VLC systems with NDLoS (pure LoS), the MIMO VLC channel matrix can be highly correlated since IM/DD has no frequency and phase information. Hence, strong correlation prevents reliable decoding of the parallel channels at the receiver [187]. Therefore, reducing the correlation of MIMO VLC channels and obtaining high spatial multiplexing gains are still important topics that need to be addressed in indoor MIMO VLCs.

C. Interference Measurements and Models

The SNR in (3) is used to evaluate link performance when disturbances are primarily related to noise that generated by the ambient light sources (the sun, fluorescence, etc). On the other hand, signal to interference ratio (SIR) and signal to interference plus noise ratio (SINR) are metrics of interest for evaluation of systems in the presence of interference from neighboring transmitters. According to central limit theorem, the interference should be normally distributed when there are no dominant interferers [188]. However, the directionality in VLC systems often leads to scenarios with dominant interferers. Furthermore, increasing the level of transmitting power is not an option to improve SINR since eye safety regulations will limit the amount of transmitting optical power. Accurate interference measurements and models for VLC networks are still missing. Hence, it is important to develop accurate interference models in order to study the overall system capacity, energy efficiency, and throughput of VLC networks.

D. 3D Channel Measurements and Models

Apart from the use 3D ray-tracing Zemax tool to model OWC channels in [76], [77], and [109], most OWC channel models were generally proposed assuming that propagation waves are traveling in two dimensions and therefore ignore the impact of the elevation angle on channel statistics. However, in reality, optical waves are propagating in three dimensions and hence the variations in both vertical and horizontal planes should be considered. 3D channel model is more accurate to characterize OWC channels, particularly for short-range communications. Thus, 3D channel measurements and models are necessary to characterize OWC channels. It seems there is a good chance to extend 3D channel models that done in RF, such as [129], [130], and [189]. However, optical properties of the surroundings need to be considered.

X. CONCLUDING REMARKS

This article has provided a survey of OWC systems in terms of evolution, features, channel scenarios, and propagation channel characteristics. Furthermore, we have comprehensively reviewed OWC channel measurements and models, primarily in the IR and visible light spectra. The main optical channel characteristics that affect the OWC link performance have been studied, including channel DC gain, RMS delay spread, frequency response, channel PL, and shadowing. The study has considered a wide range of communication environments, including indoor, outdoor, underwater, and underground. Both measurement campaigns and channel models have been classified according to the environment details, channel scenario, channel characteristics, the number of bounces, and the operating wavelength. Finally, this survey has provided future research directions that require further OWC channel measurement campaigns and developing more realistic channel models before the actual implementation.

REFERENCES

[1] C.-X. Wang *et al.*, "Cellular architecture and key technologies for 5G wireless communication networks," *IEEE Commun. Mag.*, vol. 52, no. 5, pp. 122–130, Feb. 2014.

[2] C.-X. Wang *et al.*, "Recent advances and future challenges for massive MIMO channel measurements and models," *Sci. China Inf. Sci.*, vol. 59, no. 2, pp. 1–16, Feb. 2016.

[3] A. Gupta and R. K. Jha, "A survey of 5G network: Architecture and emerging technologies," *IEEE Access*, vol. 3, pp. 1206–1232, 2015.

[4] T. S. Rappaport *et al.*, "Millimeter wave mobile communications for 5G cellular: It will work!" *IEEE Access*, vol. 1, pp. 335–349, 2013.

[5] M. Tilli *et al.*, *Handbook of Silicon Based MEMS Materials and Technologies*, 2nd ed. London, U.K.: William Andrew, 2015.

[6] S. Dimitrov and H. Haas, *Principles of LED Light Communications Towards Networked Li-Fi*. London, U.K.: Cambridge Univ. Press, 2015.

[7] R. J. Drost and B. M. Sadler, "Survey of ultraviolet non-line-of-sight communications," *J. Semicond. Sci. Technol.*, vol. 29, no. 8, pp. 1–11, Jun. 2014.

[8] Z. Xu and B. M. Sadler, "Ultraviolet communications: Potential and state-of-the-art," *IEEE Commun. Mag.*, vol. 46, no. 5, pp. 67–73, May 2008.

[9] A. R. Young, L. O. Björn, J. Moan, and W. Nultsch, *Environmental UV Photobiology*, 1st ed. New York, NY, USA: Plenum Press, 1993.

[10] Z. Ghassemlooy, W. Popoola, and S. Rajbhandari, *Optical Wireless Communications: System and Channel Modelling With MATLAB*, 1st ed. New York, NY, USA: CRC Press, 2013.

[11] M. A. Khalighi and M. Uysal, "Survey on free space optical communication: A communication theory perspective," *IEEE Commun. Surveys Tuts.*, vol. 16, no. 4, pp. 2231–2258, 4th Quart., 2014.

[12] H. Kroemer, "The double-heterostructure concept: How it got started," *Proc. IEEE*, vol. 101, no. 10, pp. 2183–2187, Oct. 2013.

[13] G. Held, *Introduction to Light Emitting Diode Technology and Applications*. New York, NY, USA: CRC Press, 2009.

[14] M. N. Khan, *Understanding LED Illumination*. New York, NY, USA: CRC Press, 2014.

[15] Y. Tanaka, S. Haruyama, and M. Nakagawa, "Wireless optical transmissions with white colored LED for wireless home links," in *Proc. IEEE PIMRC*, London, U.K., 2000, pp. 1325–1329.

[16] H. Ding, G. Chen, A. K. Majumdar, B. M. Sadler, and Z. Xu, "Modeling of non-line-of-sight ultraviolet scattering channels for communication," *IEEE J. Sel. Areas Commun.*, vol. 27, no. 9, pp. 1535–1544, Dec. 2009.

[17] Z. Xu, G. Chen, F. Abou-Galala, and M. Leonardi, "Experimental performance evaluation of non-line-of-sight ultraviolet communication systems," in *Proc. SPIE*, vol. 6709. San Diego, CA, USA, Sep. 2007, pp. 1–12.

[18] G. A. Shaw, A. M. Siegel, and J. Model, "Extending the range and performance of non-line-of-sight ultraviolet communication links," in *Proc. SPIE*, vol. 6231. Orlando, FL, USA, May 2006, pp. 1–12.

[19] R. Hou, Y. Chen, J. Wu, and H. Zhang, "A brief survey of optical wireless communication," in *Proc. AusPDC*, Sydney, NSW, Australia, 2015, pp. 41–50.

[20] A. Mahdy and J. S. Deogun, "Wireless optical communications: A survey," in *Proc. IEEE WCNC*, Atlanta, GA, USA, 2004, pp. 2399–2404.

[21] P. H. Pathak, X. Feng, P. Hu, and P. Mohapatra, "Visible light communication, networking, and sensing: A survey, potential and challenges," *IEEE Commun. Surveys Tuts.*, vol. 17, no. 4, pp. 2047–2077, 4th Quart., 2015.

[22] Y. Qiu, H.-H. Chen, and W.-X. Meng, "Channel modeling for visible light communications—A survey," *Wireless Commun. Mobile Comput.*, vol. 16, no. 14, pp. 2016–2034, Feb. 2016.

[23] Z. Zeng, S. Fu, H. Zhang, Y. Dong, and J. Cheng, "A survey of underwater optical wireless communications," *IEEE Commun. Surveys Tuts.*, vol. 19, no. 1, pp. 204–238, 1st Quart., 2017.

[24] L. Johnson, R. Green, and M. Leeson, "A survey of channel models for underwater optical wireless communication," in *Proc. IWOW*, Newcastle upon Tyne, U.K., 2013, pp. 1–5.

[25] S. Yarkan, S. Guzelgoz, H. Arslan, and R. R. Murphy, "Underground mine communications: A survey," *IEEE Commun. Surveys Tuts.*, vol. 11, no. 3, pp. 125–142, 3rd Quart., 2009.

[26] G. L. Stüber, *Principles of Mobile Communication*, 3rd ed. New York, NY, USA: Springer, 2011.

[27] A. Saha and N. Manna, *Optoelectronics and Optical Communication*. New Delhi, India: Univ. Sci. Press, 2011.

[28] T. Cevik and S. Yilmaz, "An overview of visible light communication systems," *Int. J. Comput. Netw. Commun.*, vol. 7, no. 6, pp. 139–150, Nov. 2015.

[29] V. Dixit, S. Shukla, and M. Shukla, "Performance analysis of optical IDMA system for indoor wireless channel model," in *Proc. IEEE CICN*, Mathura, India, Nov. 2012, pp. 382–386.

[30] N. Sklavos, M. Huebner, D. Goehringer, and P. Kitsos, *System-Level Design Methodologies for Telecommunication*. London, U.K.: Springer, 2014.

[31] S. Kitsinelis, *Light Sources: Basics of Lighting Technologies and Applications*, 2nd ed. New York, NY, USA: CRC Press, 2015.

[32] F. R. Gfeller and U. H. Bapst, "Wireless in-house data communication via diffuse infrared radiation," *Proc. IEEE*, vol. 67, no. 11, pp. 1474–1486, Nov. 1979.

[33] *The IrDA Standards for High-Speed Infrared Communications*. Accessed: Apr. 25, 2018. [Online]. Available: http://www.hpl.hp.com/hpjournal/98feb/feb98a2.pdf

[34] J. B. Carruthers, "Wireless infrared communications," *Wiley Encyclopedia Telecommun.*, vol. 27, no. 9, pp. 1–10, 2002.

[35] *Infrared Data Association*. Accessed: Apr. 25, 2018. [Online]. Available: http://www.irda.gov

[36] *IEEE Standard for Wireless LAN Medium Access Control (MAC) and Physical Layer (PHY) Specifications*, IEEE Standard 802.11, 1999.

[37] R. Ramirez-Iniguez, S. M. Idrus, and Z. Sun, *Optical Wireless Communications: IR for Wireless Connectivity*. New York, NY, USA: CRC Press, 2008.

[38] D. Koradecka, *Handbook of Occupational Safety and Health*. New York, NY, USA: CRC Press, 2010.

[39] L. Hanzo *et al.*, "Wireless myths, realities, and futures: From 3G/4G to optical and quantum wireless," *Proc. IEEE*, vol. 100, pp. 1853–1888, May 2012.

[40] R. Stevenson, "The LED's dark secret," *IEEE Spectr. Mag.*, vol. 46, no. 8, pp. 26–31, Aug. 2009.

[41] *Visible Light Communication Consortium (VLCC)*. Accessed: Apr. 25, 2018. [Online]. Available: http://www.vlcc.net

[42] *IEEE Standard for Local and Metropolitan Area Networks—Part 15.7: Short-Range Wireless Optical Communication Using Visible Light*, IEEE Standard 802.15.7, Sep. 2011.

[43] *PureLiFi*. Accessed Apr. 24, 2018. [Online]. Available: http://www.purelifi.com

[44] R. V. Priyan, S. Dinesh, J. Ilanthendral, and B. Ramya, "Communication system for underground mines using Li-Fi 5G technology," *Int. J. Latest Technol. Eng. Manag. Appl. Sci.*, vol. 3, no. 9, pp. 80–85, Sep. 2014.

[45] Visible Light Communications Association. (Oct. 2015). *Current Status of IEEE 802.15.7 r1 OWC Standardization*. Accessed: Apr. 25, 2018. [Online]. Available: http://www.vlca.net

[46] United States Department of Energy. *Energy Savings Forecast of Solid-State Lighting in General Illumination Applications*. Accessed: Apr. 25, 2018. [Online]. Available: http://energy.gov/eere/ssl/downloads/solid-state-lighting-2016-rd-plan

[47] T. Komine, J. H. Lee, S. Haruyama, and M. Nakagawa, "Adaptive equalization system for visible light wireless communication utilizing multiple white LED lighting equipment," *IEEE Trans. Wireless Commun.*, vol. 8, no. 6, pp. 2892–2900, Jun. 2009.

[48] R. J. Drost, T. J. Moore, and B. M. Sadler, "UV communications channel modeling incorporating multiple scattering interactions," *J. Opt. Soc. America A Opt. Image Sci. Vis.*, vol. 24, no. 4, pp. 686–695, Apr. 2011.

[49] Z. Xu and B. M. Sadler, "Performance evaluation of solar blind NLOS ultraviolet communication systems," in *Proc. Army Sci. Conf.*, Orlando, FL, USA, Dec. 2008, pp. 1–8.

[50] A. K. Majumdar, *Advanced Free Space Optics (FSO): A Systems Approach*. New York, NY, USA: Springer, 2015.

[51] D. Kedar and S. Arnon, "Subsea ultraviolet solar-blind broadband free-space optics communication," *Opt. Eng.*, vol. 48, no. 4, pp. 1–7, Apr. 2009.

[52] J. R. Barry, *Wireless Infrared Communications*. New York, NY, USA: Springer, 1994.

[53] J. M. Kahn and J. R. Barry, "Wireless infrared communications," *Proc. IEEE*, vol. 85, no. 2, pp. 265–298, Feb. 1997.

[54] Z. Ghassemlooy, *Indoor Optical Wireless Communications Systems—Part I: Review*, School Eng., Northumbria Univ., Newcastle upon Tyne, U.K., 2003.

[55] *FSONA*. Accessed: Apr. 25, 2018. [Online]. Available: http://www.fsona.com

[56] D. Wu, Z. Ghassemlooy, H. L. Minh, S. Rajbhandari, and M. A. Khalighi, "Optimisation of Lambertian order for indoor non-directed optical wireless communication," in *Proc. IEEE ICCC*, Beijing, China, Aug. 2012, pp. 43–48.

[57] O. Bouchet, *Wireless Optical Communications*. London, U.K.: Wiley, 2012.

[58] Y. A. Alqudah and M. Kavehrad, "MIMO characterization of indoor wireless optical link using a diffuse-transmission configuration," *IEEE Trans. Commun.*, vol. 51, no. 9, pp. 1554–1560, Sep. 2003.

[59] J. M. Kahn, W. J. Krause, and J. B. Carruthers, "Experimental characterization of non-directed indoor infrared channels," *IEEE Trans. Commun.*, vol. 43, nos. 2–4, pp. 1613–1623, Feb./Apr. 1995.

[60] D. P. Young *et al.*, "Diffuse mid-UV communication in the presence of obscurants," in *Proc. ASILOMAR*, Pacific Grove, CA, USA, 2012, pp. 1061–1064.

[61] V. Jungnickel, V. Pohl, S. Nonnig, and C. V. Helmolt, "A physical model of the wireless infrared communication channel," *IEEE J. Sel. Areas Commun.*, vol. 20, no. 3, pp. 631–640, Apr. 2002.

[62] D. R. Wisely, "A 1 Gbit/s optical wireless tracked architecture for ATM delivery," in *Proc. IEE Colloquium Opt. Free Space Commun. Links*, London, U.K., 1996, pp. 1–7.

[63] Y. Wang, X. Huang, J. Shi, Y.-Q. Wang, and N. Chi, "Long-range high-speed visible light communication system over 100-m outdoor transmission utilizing receiver diversity technology," *Opt. Eng.*, vol. 55, no. 5, pp. 1–8, 2016.

[64] G. Wu and J. Zhang, "Demonstration of a visible light communication system for underground mining applications," in *Proc. IECT*, Shanghai, China, Jun. 2016, pp. 1–7.

[65] K. K. Wong, T. O'Farrell, and M. Kiatweerasakul, "The performance of optical wireless OOK, 2-PPM and spread spectrum under the effects of multipath dispersion and artificial light interference," *Int. J. Commun. Syst.*, vol. 13, pp. 551–576, Nov. 2000.

[66] H. Elgala, R. Mesleh, and H. Haas, "Practical considerations for indoor wireless optical system implementation using OFDM," in *Proc. ConTEL*, Zagreb, Croatia, Jun. 2009, pp. 25–29.

[67] J. B. Carruthers and J. M. Kahn, "Modeling of nondirected wireless infrared channels," *IEEE Trans. Commun.*, vol. 45, no. 10, pp. 1260–1268, Oct. 1997.

[68] F. J. López-Hernández, R. Pérez-Jiménez, and A. Santamaria, "Ray-tracing algorithms for fast calculation of the channel impulse response on diffuse IR wireless indoor channels," *Opt. Eng.*, vol. 39, no. 10, pp. 2775–2780, Oct. 2000.

[69] M. Pätzold, *Mobile Radio Channels*, 2nd ed. Chichester, U.K.: Wiley, 2012.

[70] M. D. A. Mohamed and S. Hranilovic, "Optical impulse modulation for indoor diffuse wireless communications," *IEEE Trans. Commun.*, vol. 57, no. 2, pp. 499–508, Feb. 2009.

[71] Z. Ghassemlooy, L. N. Alves, S. Zvánovec, and M.-A. Khalighi, *Visible Light Communications Theory and Applications*. New York, NY, USA: CRC Press, 2017.

[72] D. Wu, Z. Ghassemlooy, H. Le Minh, S. Rajbhandari, and A. C. Boucouvalas, "Improvement of the transmission bandwidth for indoor optical wireless communication systems using a diffused Gaussian beam," *IEEE Commun. Lett.*, vol. 16, no. 8, pp. 1316–1319, Aug. 2012.

[73] J. Grubor, S. Randel, K.-D. Langer, and J. W. Walewsk, "Broadband information broadcasting using LED-based interior lighting," *J. Lightw. Technol.*, vol. 26, no. 24, pp. 3883–3892, Dec. 15, 2008.

[74] X. Zhang, K. Cui, M. Yao, H. Zhang, and Z. Xu, "Experimental characterization of indoor visible light communication channels," in *Proc. IEEE CSNDSP*, Poznań, Poland, Jul. 2012, pp. 1–5.

[75] J. R. Barry, J. M. Kahn, W. J. Krause, E. A. Lee, and D. G. Messerschmitt, "Simulation of multipath impulse response for indoor wireless optical channels," *IEEE J. Sel. Areas Commun.*, vol. 11, no. 3, pp. 367–379, Apr. 1993.

[76] F. Miramirkhani, M. Uysal, and E. Panayirci, "Novel channel models for visible light communications," in *Proc. SPIE*, vol. 9387. San Francisco, CA, USA, Feb. 2015, pp. 1–13.

[77] F. Miramirkhani, O. Narmanlioglu, M. Uysal, and E. Panayirci, "A mobile channel model for VLC and application to adaptive system design," *IEEE Commun. Lett.*, vol. 21, no. 5, pp. 1035–1038, May 2017.

[78] S. Dimitrov *et al.*, "Path loss simulation of an infrared optical wireless system for aircrafts," in *Proc. IEEE GLOBECOM*, Honolulu, HI, USA, Dec. 2009, pp. 1–6.

[79] J. Wang, A. Al-Kinani, J. Sun, W. Zhang, and C.-X. Wang, "A path loss channel model for visible light communications in underground mines," in *Proc. IEEE/CIC ICCC*, Qingdao, China, Oct. 2017, pp. 1–5.

[80] Y. Xiang *et al.*, "Human shadowing effect on indoor visible light communications channel characteristics," *Opt. Eng.*, vol. 53, no. 8, Aug. 2014, Art. no. 086113.

[81] M. R. Pakravan and M. Kavehrad, "Indoor wireless infrared channel characterization by measurements," *IEEE Trans. Veh. Technol.*, vol. 50, no. 4, pp. 1053–1073, Jul. 2001.

[82] S. Jivkova and M. Kavehrad, "Shadowing and blockage in indoor optical wireless communications," in *Proc. IEEE GLOBECOM*, San Francisco, CA, USA, Dec. 2003, pp. 3269–3273.

[83] S. Dimitrov *et al.*, "On the SIR of a cellular infrared optical wireless system for an aircraft," *IEEE J. Sel. Areas Commun.*, vol. 27, no. 9, pp. 1623–1638, Dec. 2009.

[84] T. Komine and M. Nakagawa, "A study of shadowing on indoor visible-light wireless communication utilizing plural white LED lightings," in *Proc. IEEE ISWCS*, Port Louis, Mauritius, Sep. 2004, pp. 36–40.

[85] R. Yuan and J. Ma, "Review of ultraviolet non-line-of-sight communication," *China Commun.*, vol. 13, no. 6, pp. 63–75, Jun. 2016.

[86] N. Hayasaka and T. Ito, "Channel modeling of nondirected wireless infrared indoor diffuse link," *J. Electron. Commun. Japan*, vol. 90, no. 6, pp. 10–19, 2007.

[87] F. J. López-Hernández and M. J. Betancor, "DUSTIN: Algorithm for calculation of impulse response on IR wireless indoor channels," *IEEE Electron. Lett.*, vol. 33, no. 21, pp. 1804–1806, Oct. 1997.

[88] H. Hashemi, G. Yun, M. Kavehrad, and F. Behbahani, "Frequency response measurements of the wireless indoor channel at infrared frequencies," in *Proc. IEEE ICCC*, New Orleans, LA, USA, 1994, pp. 1511–1515.

[89] H. Hashemi, G. Yun, M. Kavehrad, F. Behbahani, and P. Galko, "Indoor propagation measurements at infrared frequencies for wireless local area networks applications," *IEEE Trans. Veh. Technol.*, vol. 43, no. 3, pp. 562–576, Aug. 1994.

[90] G. W. Marsh and J. M. Kahn, "Performance evaluation of experimental 50-Mb/s diffuse infrared wireless link using on-off keying with decision-feedback equalization," *IEEE Trans. Commun.*, vol. 44, no. 11, pp. 1496–1504, Nov. 1996.

[91] R. Pérez-Jiménez, J. Berges, and M. J. Betancor, "Statistical model for the impulse response on infrared indoor diffuse channels," *IEEE Electron. Lett.*, vol. 33, no. 15, pp. 1298–1300, Jul. 1997.

[92] H. Hashemi, "The indoor radio propagation channel," in *Proc. IEEE*, vol. 81, no. 7, pp. 943–968, Jul. 1993.

[93] Samsung Electronics. (Jul. 2008). *VLC Channel Measurement in Indoor Applications*. Accessed: Apr. 25, 2018. [Online]. Available: http://mentor.ieee.org

[94] K. Cui, G. Chen, Z. Xu, and R. D. Roberts, "Line-of-sight visible light communication system design and demonstration," in *Proc. IEEE CSNDSP*, Newcastle upon Tyne, U.K., 2010, pp. 621–625.

[95] J. B. Carruthers and P. Kannan, "Iterative site-based modeling for wireless infrared channels," *IEEE Trans. Antennas Propag.*, vol. 50, no. 5, pp. 759–765, May 2002.

[96] D. Wu, Z. Ghassemlooy, S. Rajbhandari, and H. Le Minh, "Channel characteristics analysis and experimental demonstration of a diffuse cellular indoor visible light communication system," *Mediterr. J. Electron. Commun.*, vol. 8, pp. 1–7, Nov. 2011.

[97] P. Chvojka, S. Zvanovec, P. A. Haigh, and Z. Ghassemlooy, "Channel characteristics of visible light communications within dynamic indoor environment," *J. Lightw. Technol.*, vol. 33, no. 9, pp. 1719–1725, May 1, 2015.

[98] J. Gao, F. Yang, and X. Ma, "Indoor positioning system based on visible light communication with gray-coded identification," in *Proc. IEEE IWCMC*, Valencia, Spain, Jul. 2017, pp. 899–903.

[99] B. Lin, X. Tang, Z. Ghassemlooy, C. Lin, and Y. Li, "Experimental demonstration of an indoor VLC positioning system based on OFDMA," *IEEE Photon. J.*, vol. 9, no. 2, pp. 1–9, Apr. 2017.

[100] F. J. López-Hernández, R. Pérez-Jiménez, and A. Santamaria, "Monte Carlo calculation of impulse response on diffuse IR wireless indoor channels," *IEEE Electron. Lett.*, vol. 34, no. 12, pp. 1260–1262, Jun. 1998.

[101] F. J. López-Hernández, R. Pérez-Jiménez, and A. Santamaria, "Modified Monte Carlo scheme for high-efficiency simulation of the impulse response on diffuse IR wireless indoor channels," *IEEE Electron. Lett.*, vol. 34, no. 19, pp. 1819–1820, Sep. 1998.

[102] M. D. Higgins, R. J. Green, and M. S. Leeson, "Optical wireless for intravehicle communications: Incorporating passenger presence scenarios," *IEEE Trans. Veh. Technol.*, vol. 62, no. 8, pp. 3510–3517, Oct. 2013.

[103] V. Pohl, V. Jungnickel, and C. von Helmolt, "Integrating-sphere diffuser for wireless infrared communication," *IEE Proc. Optoelectron.*, vol. 147, no. 4, pp. 281–285, Aug. 2000.

[104] V. Pohl, V. Jungnickel, and C. von Helmolt, "A channel model for wireless infrared communication," in *Proc. IEEE PIMRC*, London, U.K., 2000, pp. 297–303.

[105] K. Smitha, A. Sivabalan, and J. John, "Estimation of channel impulse response using modified ceiling bounce model in non-directed indoor optical wireless systems," *Wireless Pers. Commun.*, vol. 45, no. 1, pp. 1–10, Apr. 2008.

[106] E. Sarbazi, M. Uysal, M. Abdallah, and K. Qaraqe, "Ray tracing based channel modeling for visible light communications," in *Proc. SPCA*, Trabzon, Turkey, Apr. 2014, pp. 23–25.

[107] E. Sarbazi, M. Uysal, M. Abdallah, and K. Qaraqe, "Indoor channel modelling and characterization for visible light communications," in *Proc. ICTON*, Graz, Austria, Jul. 2014, pp. 1–4.

[108] M. Uysal, C. Capsoni, Z. Ghassemlooy, A. Boucouvalas, and E. Udvary, *Optical Wireless Communications: An Emerging Technology*. Cham, Switzerland: Springer, 2016.

[109] F. Miramirkhani and M. Uysal, "Channel modeling and characterization for visible light communications," *IEEE Photon. J.*, vol. 7, no. 6, pp. 1–16, Dec. 2015.

[110] S. J. Lee, J. K. Kwon, S. Y. Jung, and Y. H. Kwon, "Simulation modeling of visible light communication channel for automotive applications," in *Proc. IEEE ITSC*, Anchorage, AK, USA, Sep. 2012, pp. 463–468.

[111] A. Al-Kinani, C.-X. Wang, H. Haas, and Y. Yang, "A geometry-based multiple bounce model for visible light communication channels," in *Proc. IEEE IWCMC*, Paphos, Cyprus, Sep. 2016, pp. 31–37.

[112] K. Smitha A. Sivabalan, and J. John, "Modified ceiling bounce model for computing path loss and delay spread in indoor optical wireless systems," *Int. J. Commun. Netw. Syst. Sci.*, vol. 2, no. 8, pp. 754–758, Nov. 2009.

[113] T. Komine and M. Nakagawa, "Integrated system of white LED visible-light communication and power-line communication," *IEEE Trans. Consum. Electron.*, vol. 49, no. 1, pp. 71–79, Feb. 2003.

[114] K. Lee, H. Park, and J. R. Barry, "Indoor channel characteristics for visible light communications," *IEEE Commun. Lett.*, vol. 15, no. 2, pp. 217–219, Feb. 2011.

[115] T. Komine and M. Nakagawa, "Fundamental analysis for visible-light communication system using LED lights," *IEEE Trans. Consum. Electron.*, vol. 50, no. 1, pp. 100–107, Feb. 2004.

[116] G. Ren, S. He, and Y. Yang, "An improved recursive channel model for indoor visible light communication systems," *Inf. Technol. J.*, vol. 12, no. 2, pp. 1245–1250, Apr. 2013.

[117] A. Sivabalan and J. John, "Modeling and simulation of indoor optical wireless channels: A review," in *Proc. TENCON*, Bengaluru, India, Oct. 2003, pp. 1082–1085.

[118] Z. Wang and S. Chen, "Grouped DFT precoding for PAPR reduction in visible light OFDM systems," *Int. J. Elect. Comput. Eng.*, vol. 6, no. 6, pp. 710–713, 2015.

[119] W. Wiesbeck, "The mobile to mobile (C2C) communication channel," in *Proc. IEEE EuCAP*, Edinburgh, U.K., 2007, p. 1.

[120] W. R. McCluney, *Introduction to Radiometry and Photometry*, 2nd ed. Boston, MA, USA: Artech House, 2014.

[121] *Zemax*. Accessed: Apr. 25, 2018. [Online]. Available: http://www.radiantzemax.com/zemax

[122] R. Ulbricht, *Das Kugelphotometer*. Berlin, Germany: R. Oldenbourg Verlag, 1920.

[123] S.-I. Choi, "Analysis of VLC channel based on the shapes of white-light LED lighting," in *Proc. IEEE ICUFN*, Phuket, Thailand, 2012, pp. 1–5.

[124] J. Ding, K. Wang, and Z. Xu, "Accuracy analysis of different modeling schemes in indoor visible light communications with distributed array sources," in *Proc. IEEE CSNDSP*, Manchester, U.K., Jul. 2014, pp. 1005–1010.

[125] J. B. Carruthers and S. M. Carroll, "Statistical impulse response models for indoor optical wireless channels," *Int. J. Commun. Syst.*, vol. 18, no. 3, pp. 267–284, Apr. 2005.

[126] J. B. Carruthers and P. Kannan. *IrSimIt*. Accessed: Apr. 25, 2018. [Online]. Available: http://iss.bu.edu/bwc/irsimit

[127] S. M. Carroll, "Modeling wireless infrared communications for network simulation," Ph.D. dissertation, Dept. Elect. Comput. Eng., Boston Univ., Boston, MA, USA, 2004.

[128] X. Cheng, C.-X. Wang, D. I. Laurenson, S. Salous, and A. V. Vasilakos, "An adaptive geometry-based stochastic model for non-isotropic MIMO mobile-to-mobile channels," *IEEE Trans. Wireless Commun.*, vol. 8, no. 9, pp. 4824–4835, Sep. 2009.

[129] X. Cheng, C.-X. Wang, Y. Yuan, D. I. Laurenson, and X. Ge, "A novel 3D regular-shaped geometry-based stochastic model for non-isotropic MIMO mobile-to-mobile channels," in *Proc. IEEE VTC Fall*, Ottawa, ON, Canada, Sep. 2010, pp. 1–5.

[130] Y. Yuan, C.-X. Wang, X. Cheng, B. Ai, and D. I. Laurenson, "Novel 3D geometry-based stochastic models for non-isotropic MIMO vehicle-to-vehicle channels," *IEEE Trans. Wireless Commun.*, vol. 13, no. 1, pp. 298–309, Jan. 2014.

[131] A. Al-Kinani, C.-X. Wang, H. Haas, and Y. Yang, "Characterization and modeling of visible light communication channels," in *Proc. IEEE VTC*, Nanjing, China, May 2016, pp. 1–5.

[132] M. Zhang, Y. Zhang, X. Yuan, and J. Zhang, "Mathematic models for a ray tracing method and its applications in wireless optical communications," *Opt. Exp.*, vol. 18, no. 17, pp. 18431–18437, Aug. 2010.

[133] S. R. Pérez, R. P. Jiménez, F. J. L. Hernández, O. B. G. Hernández, and A. J. A. Alfonso, "Reflection model for calculation of the impulse response on IR-wireless indoor channels using ray-tracing algorithm," *Microw. Opt. Technol. Lett.*, vol. 32, no. 4, pp. 296–300, Feb. 2002.

[134] B. T. Phong, "Illumination for computer generated pictures," *Commun. ACM*, vol. 18, no. 6, pp. 311–317, Jun. 1975.

[135] J. Giner, C. Militello, and A. García, "The Monte Carlo method to determine the error in calculation of objective acoustic parameters within the ray-tracing technique," *J. Acoust. Soc. Amer.*, vol. 110, no. 6, pp. 3081–3085, Dec. 2001.

[136] O. Gonzalez, S. Rodriguez, R. Pérez-Jiménez, B. R. Mendoza, and A. Ayala, "Error analysis of the simulated impulse response on indoor wireless optical channels using a Monte Carlo-based ray-tracing algorithm," *IEEE Trans. Commun.*, vol. 53, no. 1, pp. 124–130, Jan. 2005.

[137] D. R. Biosca, P. López, and L. Jorge, "Generalization of Monte Carlo ray-tracing algorithm for the calculation of the impulse response on indoor wireless infrared channels," *Universidad Cienciay Tecnología*, vol. 9, no. 33, pp. 17–25, 2005.

[138] D.-Q. Ding and X.-Z. Ke, "A new indoor VLC channel model based on reflection," *Optoelectron. Lett.*, vol. 6, no. 4, pp. 295–298, Jul. 2010.

[139] K. Bian, G. Zhang, and L. Song, "Toward secure crowd sensing in vehicle-to-everything networks," *IEEE Netw.*, vol. 32, no. 2, pp. 126–131, Mar./Apr. 2017.

[140] S, Zeadally, R. Hunt, Y.-S. Chen, A. Irwin, and A. Hassan, "Vehicular ad hoc networks (VANETS): Status, results, and challenges," *Telecommun. Syst.*, vol. 50, no. 4, pp. 217–241, Aug. 2012.

[141] M. Wada, T. Yendo, T. Fujii, and M. Tanimoto, "Road-to-vehicle communication using LED traffic light," in *Proc. IEEE Intell. Veh. Symp.*, Las Vegas, NV, USA, Jun. 2005, pp. 601–606.

[142] G. Pang, T. Kwan, H. Liu, and C.-H Chan, "LED wireless," *IEEE Ind. Appl. Mag.*, vol. 8, no. 1, pp. 21–28, Jan./Feb. 2002.

[143] S. Arai *et al.*, "Feasible study of road-to-vehicle communication system using LED array and high-speed camera," in *Proc. WCITS*, New York, NY, USA, 2008, pp. 1–12.

[144] M. Alam, J. Ferreira, and J. Fonseca, *Intelligent Transportation Systems: Dependable Vehicular Communications for Improved Road Safety*. Cham, Switzerland: Springer, 2016.

[145] S. Iwasaki *et al.*, "Visible light road-to-vehicle communication using high-speed camera," in *Proc. IEEE Intell. Veh. Symp.*, Eindhoven, The Netherlands, Jun. 2008, pp. 13–18.

[146] S. J. Lee, J. K. Kwon, S.-Y. Jung, and Y.-H. Kwon, "Evaluation of visible light communication channel delay profiles for automotive applications," *EURASIP J. Wireless Commun. Netw.*, vol. 2012, pp. 1–8, Dec. 2012.

[147] P. Luo *et al.*, "Performance analysis of a car-to-car visible light communication system," *Appl. Opt.*, vol. 54, no. 7, pp. 1696–1706, Mar. 2015.

[148] P. Luo *et al.*, "Bit-error-rate performance of a car-to-car VLC system using 2×2 MIMO," *Mediterranean J. Comput. Netw.*, vol. 11, pp. 400–407, Jan. 2015.

[149] A. Al-Kinani, J. Sun, C.-X. Wang, W. Zhang, and X. Ge, "A 2D non-stationary GBSM for vehicular visible light communication channels," *IEEE Trans. Wireless Commun.*, to be published.

[150] C. B. Liu, B. Sadeghi, and E. W. Knightly, "Enabling vehicular visible light communication (V2LC) networks," in *Proc. VANET*, Las Vegas, NV, USA, 2011, pp. 41–50.

[151] N. Lourenco, D. Terra, N. Kumar, L. N. Alves, and R. L. Aguiar, "Visible light communication system for outdoor applications," in *Proc. IEEE CSNDSP*, Poznan, Poland, 2012, pp. 1–6.

[152] L. Qin, Y. Zhang, K. Song, B. Li, and Y. Du, "Visible light communication system based on spread spectrum technology for intelligent transportation," *Opt. Quant. Electron.*, vol. 49, pp. 1–11, Jul. 2017.

[153] C. Gabriel, M.-A. Khalighi, S. Bourennane, P. Leon, and V. Rigaud, "Monte-Carlo-based channel characterization for underwater optical communication systems," *IEEE/OSA J. Opt. Commun. Netw.*, vol. 5, no. 1, pp. 1–12, Jan. 2013.

[154] F. Miramirkhani and M. Uysal, "Visible light communication channel modeling for underwater environments with blocking and shadowing," *IEEE Access*, vol. 6, pp. 1082–1090, 2017.

[155] N. Farr, A. Bowen, J. Ware, C. Pontbriand, and M. Tivey, "An integrated, underwater optical /acoustic communications system," in *Proc. IEEE OCEANS*, Sydney, NSW, Australia, May 2010, pp. 1–6.

[156] X. Zhang, J.-H. Cui, S. Das, M. Gerla, and M. Chitre, "Underwater wireless communications and networks: Theory and application: Part 1 [guest editorial]," *IEEE Commun. Mag.*, vol. 53, no. 11, pp. 40–41, Nov. 2015.

[157] J. H. Smart, "Underwater optical communications systems part 1: Variability of water optical parameters," in *Proc. IEEE MILCOM*, Atlantic City, NJ, USA, 2005, pp. 1140–1146.

[158] J. W. Giles and I. N. Bankman, "Underwater optical communications systems. Part 2: Basic design considerations," in *Proc. IEEE MILCOM*, Atlantic City, NJ, USA, 2005, pp. 1700–1705.

[159] B. Cochenour, L. Mullen, and J. Muth, "Temporal response of the underwater optical channel for high-bandwidth wireless laser communications," *IEEE J. Ocean. Eng.*, vol. 38, no. 4, pp. 730–742, Oct. 2013.

[160] H. Kaushal and G. Kaddoum, "Underwater optical wireless communication," *IEEE Access*, vol. 4, pp. 1518–1547, 2016.

[161] B. M. Cochenour, L. J. Mullen, and A. E. Laux, "Characterization of the beam-spread function for underwater wireless optical communications links," *IEEE J. Ocean. Eng.*, vol. 33, no. 4, pp. 513–521, Oct. 2008.

[162] S. Jaruwatanadilok, "Underwater wireless optical communication channel modeling and performance evaluation using vector radiative transfer theory," *IEEE J. Sel. Areas Commun.*, vol. 26, no. 9, pp. 1620–1627, Dec. 2008.

[163] J. R. Potter, M. B. Porter, and J. C. Preisig, "UComms: A conference and workshop on underwater communications, channel modeling, and validation," *IEEE J. Ocean. Eng.*, vol. 38, no. 4, pp. 603–613, Oct. 2013.

[164] V. Guerra, C. Quintana, J. Rufo, J. Rabadan, and R. Perez-Jimenez, "Parallelization of a Monte Carlo ray tracing algorithm for channel modelling in underwater wireless optical communications," *Procedia Technol.*, vol. 7, pp. 11–19, 2013.

[165] V. Guerra, O. El-Asmar, C. Suarez-Rodriguez, R. Perez-Jimenez, and J. M. Luna-Rivera, "Statistical study of the channel parameters in underwater wireless optical links," in *Proc. IEEE IWOBI*, Liberia, Costa Rica, 2014, pp. 124–127.

[166] W. Liu, D. Zou, P. Wang, Z. Xu, and L. Yang, "Wavelength dependent channel characterization for underwater optical wireless communications," in *Proc. IEEE ICSPCC*, Guilin, China, 2014, pp. 895–899.

[167] W. Liu, D. Zou, Z. Xu, and J. Yu, "Non-line-of-sight scattering channel modeling for underwater optical wireless communication," in *Proc IEEE CYBER*, Shenyang, China, 2015, pp. 1265–1268.

[168] Y. Dong and J. Liu, "On BER performance of underwater wireless optical MISO links under weak turbulence," in *Proc. IEEE/MTS OCEANS*, Shanghai, China, Apr. 2016, pp. 1–4.

[169] H. Zhang, Y. Dong, and X. Zhang, "On stochastic model for underwater wireless optical links," in *Proc. IEEE ICCC*, Shanghai, China, 2014, pp. 156–160.

[170] H. Zhang and Y. Dong, "General stochastic channel model and performance evaluation for underwater wireless optical links," *IEEE Trans. Wireless Commun.*, vol. 15, no. 2, pp. 1162–1173, Feb. 2016.

[171] J. B. Snow *et al.*, "Underwater propagation of high-data-rate laser communications pulses," in *Proc. SPIE*, vol. 1750. San Diego, CA, USA, Dec. 1992, pp. 419–427.

[172] J. W. Bales and C. Chryssostomidis, "High-bandwidth, low-power, short-range optical communication underwater," in *Proc. UST*, Durham, NH, USA, 1995, pp. 406–415.

[173] F. Hanson and S. Radic, "High bandwidth underwater optical communication," *Appl. Opt.*, vol. 47, no. 2, pp. 277–283, 2008.

[174] W. Cox and J. Muth, "Simulating channel losses in an underwater optical communication system," *J. Opt. Soc. Amer. A.*, vol. 31, no. 5, pp. 920–934, 2014.

[175] C. Li, K.-H. Park, and M.-S. Alouin, "On the use of a direct radiative transfer equation solver for path loss calculation in underwater optical wireless channels," *IEEE Commun. Lett.*, vol. 4, no. 5, pp. 561–564, Oct. 2015.

[176] J. Wang, A. Al-Kinani, W. Zhang, and C.-X. Wang, "A new VLC channel model for underground mining environments," in *Proc. IEEE IWCMC*, Valencia, Spain, Jun. 2017, pp. 2134–2139.

[177] P. Ren and J. Qian, "A power-efficient clustering protocol for coal mine face monitoring with wireless sensor networks under channel fading conditions," *Sensors*, vol. 16, no. 6, pp. 1–21, Jun. 2016.

[178] Y. Zhang, Y. Zhang, and C. Li, "Research of short distance wireless communication technology in the mine underground," in *Proc. IMCCC*, Harbin, China, Sep. 2014, pp. 955–959.

[179] B. A. Vijayalakshmi and M. N. Sudha, "Illumination and communication using LED as light source in underground mines," in *Proc. ICIIT*, Chennai, India, Dec. 2017, pp. 171–178.

[180] Y. Zhai and S. Zhang, "Visible light communication channel models and simulation of coal workface energy coupling," *IEEE J. Math. Problems Eng.*, vol. 2015, pp. 1–10, Nov. 2015.

[181] J. Wang *et al.*, "A path loss channel model for visible light communications in underground mines," *China Commun.*, vol. 14, no. 8, Aug. 2018.

[182] E. Cole. (2016, Feb). *Boeing, University Teams Apply AI to Aircraft Safety*. Accessed: Apr. 25, 2018. [Online]. Available: https://www.roboticsbusinessreview.com/manufacturing/boeing_university_teams_apply_ai_to_aircraft_safety

[183] G. Corbellini, K. Aksit, S. Schmid, S. Mangold, and T. R. Gross, "Connecting networks of toys and smartphones with visible light communication," *IEEE Commun. Mag.*, vol. 52, no. 7, pp. 72–78, Jul. 2014.

[184] D. R. Dhatchayeny, W. A. Cahyadi, S. R. Teli, and Y.-H. Chung, "A novel optical body area network for transmission of multiple patient vital signs," in *Proc. IEEE ICUFN*, Milan, Italy, Jul. 2017, pp. 542–544.

[185] I.-C. Lu, Y.-L. Liu, and C.-H. Lai, "High-speed 2×2 MIMO-OFDM visible light communication employing phosphorescent LED," in *Proc. IEEE ICUFN*, Vienna, Austria, 2016, pp. 222–224.

[186] A. Nuwanpriya, S.-W. Ho, and C. S. Chen, "Indoor MIMO visible light communications: Novel angle diversity receivers for mobile users," *IEEE J. Sel. Areas Commun.*, vol. 33, no. 9, pp. 1780–1792, Sep. 2015.

[187] F. Bohagen, P. Orten, and G. E. Oien, "Design of optimal high-rank line-of-sight MIMO channels," *IEEE Trans. Wireless Commun.*, vol. 6, no. 4, pp. 1420–1425, Apr. 2007.

[188] M. Rahaim and T. D. C. Little, "Optical interference analysis in visible light communication networks," in *Proc. IEEE ICCW*, London, U.K., 2015, pp. 1410–1415.

[189] Y. Liu *et al.*, "Channel measurements and models for high-speed train wireless communication systems in tunnel scenarios: A survey," *Sci. China Inf. Sci.*, vol. 60, no. 8, Oct. 2017, Art. no. 101301.

Ahmed Al-Kinani received the B.Sc. degree (Hons.) in laser physics and the M.Sc. degree in optical communications from the University of Technology, Baghdad, Iraq, in 2001 and 2004, respectively, and the Ph.D. degrees in optical wireless communications from the University of Edinburgh and Heriot-Watt University, Edinburgh, U.K., in 2018. He is currently with the Iraqi Ministry of Communications, Baghdad, as a Senior Programmer. His main research interests include wireless channel characterization and modeling for visible light communications.

Cheng-Xiang Wang (S'01–M'05–SM'08–F'17) received the B.Sc. and M.Eng. degrees in communication and information systems from Shandong University, China, in 1997 and 2000, respectively, and the Ph.D. degree in wireless communications from Aalborg University, Denmark, in 2004.

He was a Research Assistant with the Hamburg University of Technology, Hamburg, Germany, from 2000 to 2001, a Research Fellow with the University of Agder, Grimstad, Norway, from 2001 to 2005, and a Visiting Researcher with Siemens AG-Mobile Phones, Munich, Germany, in 2004. He has been with Heriot-Watt University, Edinburgh, U.K., since 2005, where he became a Professor in wireless communications in 2011. He is also an Honorary Fellow with the University of Edinburgh, U.K., a Chair Professor of Shandong University, and a Guest Professor of Southeast University, China. He has co-authored two books, one book chapter, and over 320 papers in refereed journals and conference proceedings. His current research interests include wireless channel measurements/modeling and (B)5G wireless communication networks, including green communications, cognitive radio networks, high mobility communication networks, massive MIMO, millimeter wave communications, and visible-light communications.

He was a recipient of Nine Best Paper Awards from IEEE GLOBECOM 2010, IEEE ICCT 2011, ITST 2012, IEEE VTC 2013-Spring, IWCMC 2015, IWCMC 2016, IEEE/CIC ICCC 2016, and WPMC 2016 and a Highly Cited Researcher Award by Web of Science in 2017. He has served as a technical program committee (TPC) member, the TPC chair, and a general chair for over 80 international conferences. He has served as an Editor for nine international journals, including the IEEE Transactions on Wireless Communications from 2007 to 2009, has been serving as an Editor for the IEEE Transactions on Vehicular Technology since 2011, and the IEEE Transactions on Communications since 2015. He was the Lead Guest Editor of the IEEE Journal on Selected Areas in Communications Special Issue on Vehicular Communications and Networks. He was also a Guest Editor of the IEEE Journal on Selected Areas in Communications Special Issue on Spectrum and Energy Efficient Design of Wireless Communication Networks and Special Issue on Airborne Communication Networks, and a Guest Editor of the IEEE Transactions on Big Data Special Issue on Wireless Big Data. He is a fellow of the IET and HEA.

Li Zhou received the B.Sc. and M.E. degrees in electrical engineering from Shandong University, China, in 1998 and 2001, respectively, and the Ph.D. degree in electrical engineering from Zhejiang University, Hangzhou, China, in 2004. She was a Project Manager with Freescale Semiconductor Research and Development Center until 2009. Since 2009, she has been an Assistant Professor with Shandong University, China. She participated in multiple National high-technology SoC and HDTV fundamental research projects, led multiple 65-nm/90-nm 10 million gate scale VLSI SoC chips, and joined many VLSI project and architecture researches. Her current research interests include visible light communication system design and evaluations, video processing system and hardware design, GPU architecture and VLSI design, embedded system, and ASIC design.

Wensheng Zhang received the M.E. degree in electrical engineering from Shandong University, China, in 2005, and the Ph.D. degree in electrical engineering from Keio University, Japan, in 2011. In 2011, he joined the School of Information Science and Engineering, Shandong University, where he is currently an Associate Professor. His research interests lie in cognitive radio networks, random matrix theory, and visible light communications.